A Review of Partial Discharge in Stator Winding of Rotating Machines Fed by Voltage Source PWM Motor Drives

Sama Salehi Vala, *Graduate Student Member, IEEE*, Abdul Basit Mirza, *Graduate Student Member, IEEE*, Asif Imran Emon, *Member, IEEE*, and Fang Luo, *Senior Member, IEEE*

***Abstract*—Partial Discharge (PD) is a critical threat to insulation reliability in rotating machines fed with Voltage Source Pulse Width Modulation (VS-PWM) motor drives. With the growing adoption of VS-PWM drives in electrified systems, driven by the fast-switching capability and efficiency benefits offered by Wide Band Gap (WBG) devices, it is imperative to design motor stator windings with robust and PD-free insulation. This comprehensive review focuses on elucidating the influence of PWM voltage waveform characteristics of VS-PWM motor drives on PD phenomena, exploring factors such as rise time, frequency, pulse width, voltage shape, and dead time. Additionally, the paper delves into potential reasons explaining the differences in results across various literature and emphasizes the need for a standardized test procedure and setup. Furthermore, the paper reviews various methods adopted in the literature to detect, separate, and quantify PD events under switching frequencies and *dv/dt* environments. By examining these aspects, this paper contributes to understanding the intricate relationship between VS-PWM drive output voltage and PD-induced stator winding insulation degradation.**

***Index Terms*—Motor drives, partial discharge (PD), PD detection methods, pulse width modulation (PWM), rotating machines, stator winding, voltage source, voltage waveform characteristics, wide band gap (WBG).**

I. Introduction

DECREASING air quality has been a worldwide concern for years, and electrification of systems is one of the proposed approaches to alleviate the problem [1]. The exploration of solutions in the realm of electrification began with transportation systems, such as electric vehicles, and has subsequently extended to include the aviation and naval industries [2]. In the endeavor towards electrification and the transition from conventional fuel-consuming transportation systems to those powered by renewable energy sources, electric drives play a pivotal role in propelling electric motors [3].

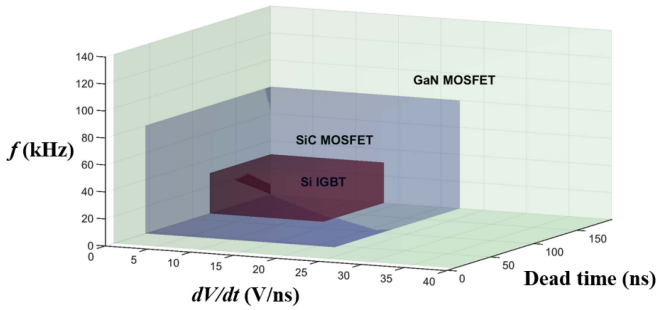

Fig. 1. Si, SiC, and GaN device characteristics [5], [6], [7], [8], [9].

VS-PWM motor drives, utilizing silicon (Si) insulated-gate bipolar transistors (IGBTs) or thyristors, have been extensively investigated and employed as variable speed drives (VSDs) for electric machines to enhance system performance and efficiency [4]. However, the landscape has evolved with the emergence of WBG devices, particularly Silicon Carbide (SiC) and more recently Gallium Nitride (GaN). These advanced WBG devices surpass their Si counterparts in crucial aspects such as switching speeds (*dv/dt*), frequency, and dead time (depicted in Fig. 1). At present, SiC devices are more widely used in high-voltage and high-power VS-PWM drives, as they are more mature than Gallium Nitride (GaN) for voltage levels above 650 V [5].

However, with widespread adoption of VS-PWM motor drive for the control of motors, an apparent correlation has emerged, linking the utilization of these drives to instances of premature motor failures. These failures are predominantly attributed to partial discharges (PDs), a consequence of heightened electrical stresses [10], [11], [12], [13]. This phenomenon is defined as "localized electrical discharges that only partially bridge the insulation between conductors, which may or may not occur adjacent to a conductor" as articulated by [14].

Common applications of PWM voltage waveforms to feed and control electric motors considerably increase degradation pace of their winding insulation, as compared with the traditional 50/60 Hz sinusoidal voltage supply, and the pulse voltage

Manuscript received 31 August 2023; revised 26 November 2023; accepted 19 December 2023. Date of publication 22 January 2024; date of current version 21 May 2024. Paper 2023-EMC-0959.R1, presented at the 2022 IEEE Transportation Electrification Conference & Expo, Anaheim, CA, USA, Jun. 15–17, and approved for publication in the IEEE TRANSACTIONS ON INDUSTRY APPLICATIONS by the Electric Machines Committee of the IEEE Industry Applications Society [DOI: 10.1109/ITEC53557.2022.9814056]. This work was supported in part by the National Science Foundation under Grant 1846917, and in part by Federal Aviation Administration under Grant 692M15-20-C-00010. *(Corresponding author: Sama Salehi Vala.)*

The authors are with the Electrical and Computer Engineering, Stony Brook University, Stony Brook, NY 11794 USA (e-mail: sama.salehivala@stonybrook.edu; abdulbasit.mirza@stonybrook.edu; asifimran.emon@stonybrook.edu; fang.luo@stonybrook.edu).

Color versions of one or more figures in this article are available at https://doi.org/10.1109/TIA.2024.3356488.

Digital Object Identifier 10.1109/TIA.2024.3356488

stress on the insulation system (particularly on the inter-turn insulation) of inverter-fed motors is different from the power-frequency voltage stress. This phenomenon is attributed to two main reasons.

Firstly, transient voltage overshoots due to traveling waves, or Reflected Wave (RW) phenomenon, caused by an impedance mismatch between the motor and cable can lead to overvoltage up to two times the DC-link voltage, exacerbating the PD phenomenon. the amplitude of the overshoot or spike is contingent upon the cable length and the rise time of the pulse voltage wave. Typically, longer cable lengths result in more pronounced overshoots or spikes. Additionally, the repetitive frequency of these spikes is directly proportional to the switching frequency of the inverter [15], [16], [17], [18], [19], [20]. Moreover, increasing the switching frequency can further intensify the RW phenomenon due to double pulsing [21].

Secondly, an examination of surges applied to randomly wound stator windings by VS-PWM drives reveals that these surges may encompass frequency components reaching up high frequencies, above 5 MHz. At such elevated frequencies, the stator windings manifest as a complex ladder network with low-impedance capacitive shunts to ground. These capacitive shunts result in a substantial portion of the applied surge voltage being distributed across the initial turns in a stator winding and potentially crossing the Partial Discharge Inception Voltage (PDIV) level. Consequently, the nonuniform voltage distribution among the turns within a coil is identified as the causative factor for the PD degradation of interturn insulation. This degradation, normally absent under standard sinusoidal power frequency voltage, is found to be notably pronounced in randomly wound motors [22], [23], [24]. Further, the uneven voltage distribution concerns are more exacerbated in a SiC device-based motor drive compared to a Si device-based system [21], [25]. This is attributed to fast-switching capability of SiC devices (Fig. 1).

Research has delved into PD in motor windings under voltage stress, considering various parameters, including voltage waveform shape [20], [21], [22], voltage polarity [23], voltage pulse repetitive rate [23], [24], and voltage rise/fall time [21], [24], [25], [26], [27]. Given the crucial importance of validating insulation systems and their resistance to PD in rotating electrical machines fed from voltage converters, organizations such as the International Electrotechnical Commission (IEC) have established standards to qualify motor insulations, ensuring their reliable operation with VSDs, IEC 60034-18-41 and IEC 60034-18-42 [18], [20]. Type I insulation materials, specified in [18], are generally used in random wound motors and are not expected to withstand PD activity during their regular operation due to the vulnerability to PD attack of the very thin organic insulation material. However, Type II insulation materials are often rated for voltages higher than Type I and preferred in form wound motors. Further, motors with Type II insulation material can experience moderate PD during their service time [20].

These two standards provide a series of test procedures to evaluate the motors' insulation, fed with a VS-PWM drive, to ensure that the PDIV or Repetitive Partial Discharge Inception Voltage (RPDIV) is high enough to guarantee the safe performance of the motors driven by VSDs. RPDIV is defined in IEC 61934 as the minimum peak to peak voltage that gives rise to at least five PD events in every ten voltage impulses [26]. However, the accuracy of the presented off-line tests is questionable since the exact stress that motor insulation experiences during the operation cannot be measured accurately. Therefore, based on [27], using standards with the off-line test procedure can lead to motors with damaged insulation material being qualified as healthy or vice versa.

As per the majority of prevailing standards assessing the insulation reliability of a system can be made more cost-effective and efficient by employing a sinusoidal voltage source with the same peak-to-peak voltage as a PWM voltage source. This streamlined approach yields equivalent results to applying the PWM voltage while reducing the complexities associated with test setup. This presumption underscores that the waveform characteristics (shape) of the supply voltage do not alter the pattern of PD events. In essence, the key determinants for PD tests are the lifetime of the insulation and the peak-to-peak voltage. To evaluate this proposition, comprehensive investigations into the influence of waveform characteristics on PD within motor winding insulation have been conducted and documented in the literature. Among these research findings, it is elucidated that factors such as rise time, frequency, duty cycle, voltage shape, and deadtime can have a more pronounced impact on insulation lifespan than the mere peak-to-peak voltage.

Moreover, existing studies for PD investigation in motors commonly utilize pulsed voltage sources with predominantly Si and, more recently, SiC-based semiconductor devices. However, as manufacturing processes mature and advance for high-voltage GaN devices, coupled with the emergence of Ultra-WBG semiconductors, the switching dv/dt for next-generation VS-PWM drives is anticipated to increase significantly. Consequently, the impact of these heightened dv/dt values on PD behavior requires thorough investigation.

This paper provides a comprehensive examination of various factors associated with PWM voltages and their influence on PD and insulation lifespan in rotating machines, as documented in the literature [28]. Section II presents different types of stator windings, a brief review of turn-to-turn PD test sample selection according to IEC 60034-18-41 and IEC 60034-18-42. Additionally, this section delves into the rationale behind the prevalent use of twisted wires in the literature for turn-to-turn insulation, shedding light on the motivations behind this common selection. In Section III, the paper explores the impact of various waveform characteristics, encompassing rise time, duty cycle, voltage waveform shape, frequency, and dead time, on PD behavior in a range of both Si and WBG (SiC-based) motor drives. Furthermore, Section IV discusses techniques for detecting PD, employed in the literature. This section also underscores the challenges encountered in PD detection within environments characterized by high dv/dt. Lastly, Section V brings the paper to a conclusion, encapsulating the key findings and insights presented throughout the study.

II. Classification of Stator Windings and PD Test Sample Selection

The literature commonly categorizes stator windings into two or three types: random wound windings, form wound windings,

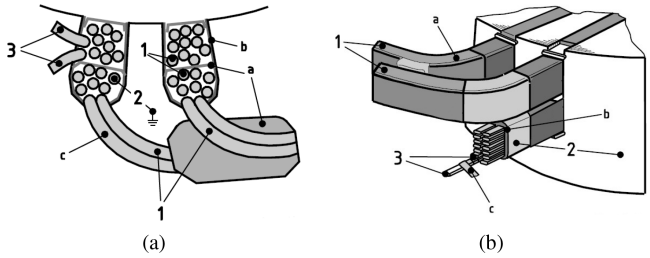

Fig. 2. Example of a motor winding design (a) random wound winding (b) form wound winding [20]. 1: Phase to phase. 2: Phase to ground. 3: Turn to turn (a) phase/overhand insulation. (b) copper conductors and stator core insulation. (c) turn insulation.

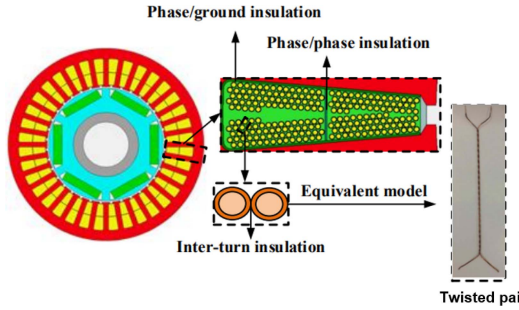

Fig. 3. Insulation system of a PMSM motor and PD test sample [32].

and Roebel bar windings [29]. Random wound windings use round cross-section wires, while form and Roebel windings utilize flat (rectangular) wires. Despite their differences in winding configurations, it is widely acknowledged that form and Roebel windings can be regarded as a single type of winding.

In a random wound winding, illustrated in Fig. 2(a), the arrangement of each turn within the coil can be arbitrary, lacking any specific order or pattern, which is the reason that they are named random wound windings. Due to the limited withstand voltage of thin insulation coatings, random wound machines are frequently utilized for low voltage applications. Conversely, in form wound windings, as depicted in Fig. 2(b), the stator slots are completely filled with a resin-based insulation material, effectively anchoring the winding strands in place. This type of winding is commonly adopted in high voltage machines with ratings surpassing 1000 V r.m.s. [30], [31].

It is crucial to recognize that, despite having higher-rated voltage and superior resistance to partial discharges, form wound motor windings are typically not deemed preferable for electric vehicles and aviation applications when compared to random wound motors. This preference is primarily due to the increased weight, cost, and higher copper loss at high speeds associated with form wound motors [31], [32].

In low-voltage windings, whether random or form-wound, the insulation around the conductor is typically thin, and there is often some air surrounding the wire, as mentioned in IEC 60034-18-41, [18]. Furthermore, in random wound windings, it's common for the first and last turns of one or more coils to be adjacent. When there is sufficient electric stress, the air between the wires or to the ground may undergo electrical breakdown, resulting in a spark or PD in the air. The electrons and ions produced by the discharge in the air then bombard the wire, ground, or phase insulation.

In random wound windings, the insulation for the wire is a thin organic film. Over time, the PD gradually erodes this film, ultimately leading to insulation failure and a shorted coil. Consequently, the turn-to-turn insulation is identified as the most susceptible to PD and [18] designates twisted pairs as standardized and simplified representations of random motor windings for PD tests.

Conversely, to test the turn-to-turn insulation system with Type II insulation material, standard IEC 60034-18-42 recommends using specimens consisting of moterettes or full winding for random wound windings and for form wound windings tests, specimen should consist of coils or bars.

Given the susceptibility of turn-to-turn insulation in random wound windings motors, substantial research has concentrated on this aspect. However, additional research is needed to address Type II insulation in rotating machinery, following the guidelines outlined in IEC 60034-18-42.

To elaborate on the rationale behind choosing twisted wires for turn-to-turn insulation by [18] and literature, Fig. 3 illustrates the cross-section of the Permanent Magnet Synchronous Machine (PMSM) with random wound winding designed by [32]. This depiction showcases the insulations for phase-to-ground, phase-to-phase, and turn-to-turn configurations. Particularly noteworthy is the presence of two thin layers of insulation within each stator slot, coating the adjacent conductors. This arrangement closely resembles the configuration of wires in a twisted pair, emphasizing the deliberate choice of this design for turn-to-turn insulation.

However the accuracy of PD test result using twisted wires and full winding placed in the slot of the motor questioned. Detecting PD between inter-turn insulation poses a formidable technical obstacle. Based on the literature, while ultra-high-frequency (UHF) sensors, such as d-dot antennas, are highly sensitive to PD pulses, inter-turn PD signals within winding insulation can undergo substantial attenuation during transmission. This attenuation results from notable losses in high-frequency signals and the electromagnetic shielding effects of the motor structure. Installing a UHF sensor externally may lack the required sensitivity to detect PD activity between interturn insulation under repetitive pulse voltage. Integrating a conventional UHF antenna inside a medium or low voltage motor proves challenging due to the restricted available space. Therefore, many studies employ twisted pairs for wire and winding insulation assessments, a practice consistent with guidelines outlined in IEC 60034-18-41 [23].

The IEC 60851-5 standard, referenced as [33], is the primary guideline for preparing PD test samples involving twisted wires, as commonly found in the literature. This standard outlines the specific quantity of twists and the length of the twisted segment of wires to ensure accurate and consistent PD testing.

Further in extension to twisted pairs, several publications, such as [34], [35], [36], [37], opt for crossed wires also, considering them simplified versions with only a single contact point. This preference is reinforced by investigations in [38], indicating

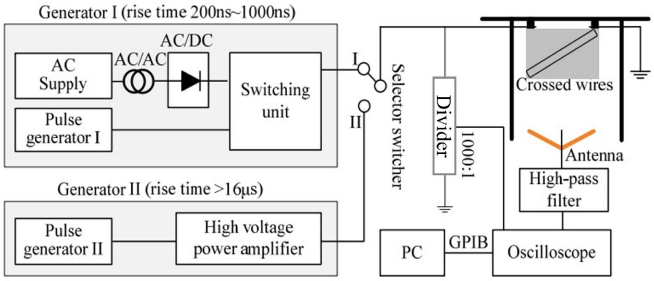

Fig. 4. Tests setup for evaluation of the effect of rise time on PD [34].

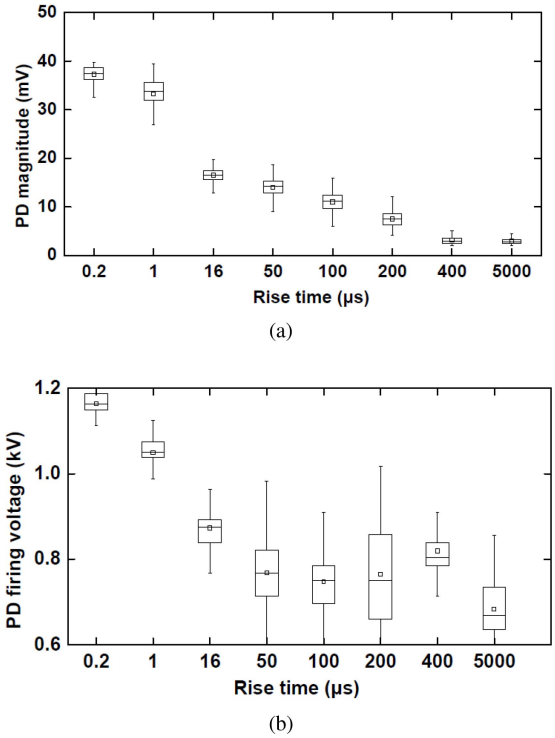

Fig. 5. Effect of rise time on (a) PD magnitude, (b) PD firing voltage [34].

that the PD mechanism in crossed samples closely mirrors that of twisted ones.

In the context of this paper, which aims to evaluate the impact of PWM characteristics on PD patterns in the interturn insulation of random wound winding motors, the primary selection of test samples revolves around twisted pairs and crossed wires.

III. Impact of PWM Waveform Characteristics on PD Pattern

This section is devoted to examining the influence of several parameters of PWM voltage pulses on different aspects of PD, such as PDIV and RPDIV. These parameters encompass various factors related to the voltage waveform generated by the motor drives, including rise time, frequency, duty cycle, voltage waveform shape, and deadtime, spanning from IGBT to WBG device ranges.

A. Rise Time

To investigate the impact of rise time on PD, RPDIV, and PDIV, [34] employs two voltage generators capable of generating bipolar voltage pulses with varying rise times. The first generator is IGBT based and generates square wave voltages with rise times ranging from 200 ns to 1 μs, while the second generator, which is a Trek 30/20 high voltage power amplifier, produces square wave voltages with rise times higher than 16 μs. Fig. 4 illustrates the test setup utilized in [34], where crossed wires are employed as the test sample to simulate turn-to-turn insulation in motor windings. To detect PD events, a horn antenna is utilized to capture the electromagnetic emissions associated with PD activities.

Using the test setup depicted in Fig. 4, a series of tests are conducted, where the rise time is swept from 0.2 μs to 400 μs, while keeping other parameters such as peak-to-peak voltage, frequency, and duty cycle fixed at 2.5 kV, 50 Hz, and 50%, respectively. Additionally, a sinusoidal voltage with the same peak-to-peak voltage and a rise time of approximately 5000 μs is employed to dissect the effect of prolonged rise time on PD patterns. Fig. 5(a) illustrates the impact of rise time on the magnitude of PD events, while Fig. 5(b) depicts the variation of the PD firing voltage with increasing rise time. The firing voltage is defined as the instantaneous voltage, occurring after the PDIV is reached, at which PD takes place [34].

The test results lead to the conclusion that for higher rise times or slower slew rate, firing voltage decreases, while faster rise times correspond to higher firing voltages. This observation can be justified by considering that PD events occur with statistical delays after PDIV is reached. While a shorter rise time gives rise to higher overvoltage, which, in turn, causes the PD firing voltage of square voltages with shorter rise times to be higher. Moreover, higher firing voltage of fast rise times induces PDs with higher magnitudes [34], [39].

Likewise, tests conducted by [40] demonstrate that increasing rise time leads to a decrease in the PDIV value. This study employs twisted pairs as the PD test samples, a Photomultiplier Tube (PMT) as the PD detection system, and pulse voltage generators, based high voltage semiconductor switch, capable of generating negative single surge voltages. Fig. 6 illustrates the negative pulse voltage for various rise times and how it impacts the magnitude of the PD, and Fig. 7 displays the corresponding PDIV for range of rise times.

To theoretically validate the test results, this reference examines the initial electrons generation probability, which induce PD under high electric field and short rise time of surge voltage, by means of Volume-Time theory to estimate the PDIV value for voltage waveforms with different rise times. In the context of the Volume-Time theory, "volume" refers to the region with a high electric field, while "time" corresponds to the duration of exposure to this high electric field. The PDIV calculated using the Volume-Time theory closely corresponds with the experimentally determined PDIV for waveforms with different rise times. This alignment serves to validate the results obtained from the experimental observations [40].

Furthermore, an exhaustive study is conducted by [41] to investigate the effect of rise time on PD patterns. The PD test

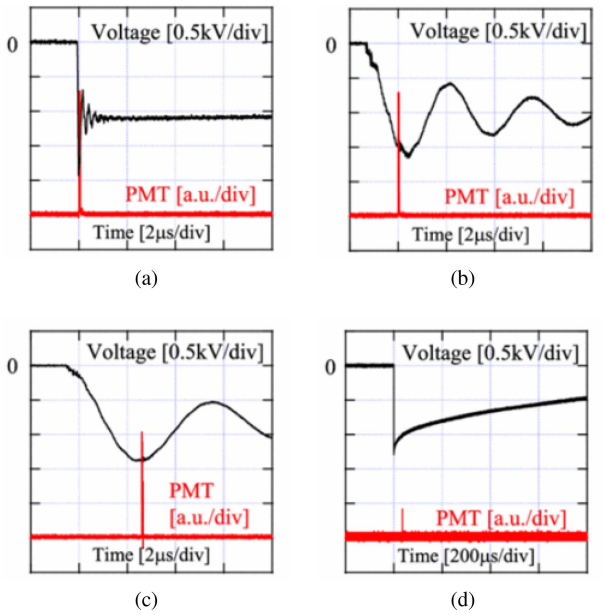

Fig. 6. Effect of rise time on PDIV (a) Surge I, (b) Surge IV, (c) Surge V, (d) Impulse [40].

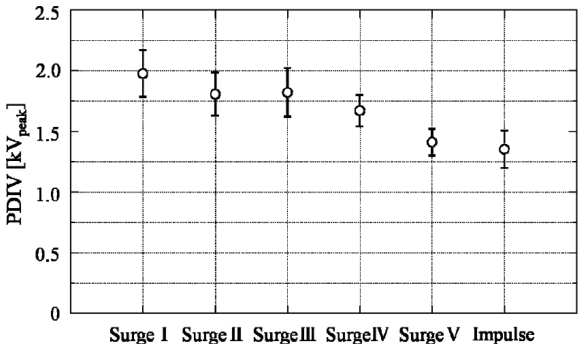

Fig. 7. Effect of rise time on PDIV [40].

results presented in this reference reveal that a shorter rise time leads to PD activities characterized by higher magnitudes, consistent with the observations in [34]. Phase-resolved PD (PRPD) analyses are performed for the regular three-level and smoothed three-level configurations generated by MOSFETs, as depicted in Fig. 8. Given the diminished occurrence of PD events and their magnitudes, an increase in the rise time of flanks is proposed as a solution to reduce PD exposure in motor windings.

As can be observed from Fig. 8, the rise time has only been increased for the first flank after the polarity change, while for the other flanks, the rise time has remained the same, 0.4 μs. The evidence presented in Table I demonstrates that augmenting the rise time can effectively contribute to the management and mitigation of PD parameters such as summed PD (sum of amplitudes of PD events), the highest PD magnitude, and the count of events calculated per cycle.

In the continuation of investigation on the effect of rise time on PD, [41] has performed a similar study on a four-level inverter, and the observations are summarized in Table II. Rise times

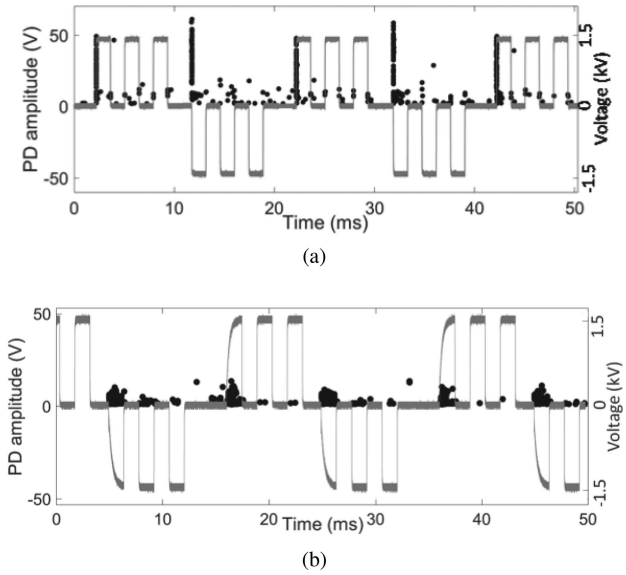

Fig. 8. PRPD for (a) regular three level PWM waveform with 0.4 μs rise time, (b) improved three level PWM waveform with increased rise time to 500 μs [41].

TABLE I
PD CHARACTERISTICS ACHIEVED PER MODULATED CYCLE FOR VARIOUS RISE TIMES [41]

Level	Rise Time (us)	Sum PD (V)	Average max PD (V)	Number of PDs
3	0.4	480	51	95
3	100	140	16	49
3	500	54	5.8	59
Sinusoidal	6670	50	6.1	29

TABLE II
PD CHARACTERISTICS ACHIEVED PER MODULATED CYCLE FOR VARIOUS RISE TIMES [41]

Level	Rise Time (us)	Sum PD (V)	Average max PD (V)	Number of PDs
4	0.4	251	26	55
4	20	91	20	66
4	20*	78	9	60
4	100	60	14	62
4	100*	48	7	59
4	500	52	6.8	39
4	500*	31	6	29

noted with * in Table II shows another layer of modification on the PWM waveform of the four-level inverter in which rather than the first pulse in each voltage level, the rise time for pulses with polarity reversal is also increased as it can be observed from Fig. 9 and Table II, this solution further decreases the PD parameters and could be considered as an approach for PD mitigation.

However, practical test results from [42] demonstrate lack of correlation between voltage rise time and the PDIV value. This reference attributes these observations to two distinct factors. Firstly, considering the generation probability of initial electrons within the wedge-shaped gap of the twisted pair specimen, an increase in rise time would correspond to a decrease in the PDIV. Conversely, when considering factors such as surge impedance

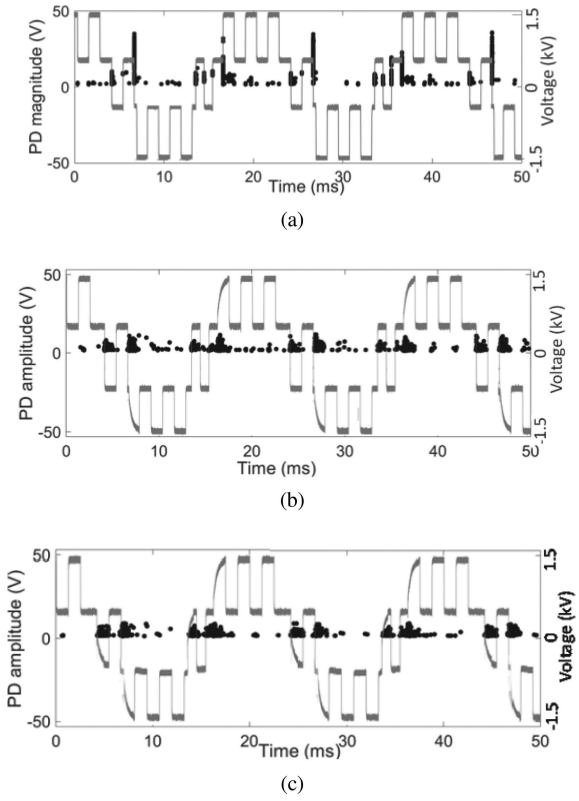

Fig. 9. PRPD for (a) regular four level PWM waveform with 0.4 μs rise time, (b) improved four level PWM waveform with increased rise time to 500 μs for the first pulse in each voltage level, (c) further improved four level PWM waveform with increased rise time to 500 μs for the first pulse and pulse with polarity reversal [41].

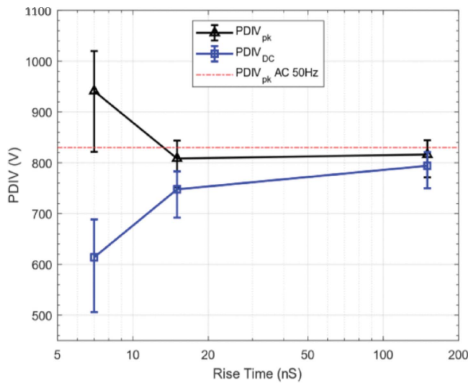

Fig. 10. Dependence of PDIV as function of rise time [43].

mismatch, traveling wave characteristics, and various aspects related to the sample and circuit configurations, an increase in rise time would lead to an increase in PDIV. Therefore, the test results are justified by the neutralizing effect of these two conflicting factors.

Similarly, [43] delves into the impact of the fast rise time of SiC devices (MOSFETs) on PD patterns in windings, utilizing a twisted pair as the test sample. The study reports that PD tests under 10 kHz reveal no discernible relationship between PDIV and rise time. The results are illustrated in Fig. 10, presenting both the peak voltage and the DC bus voltage for fast-rising pulse

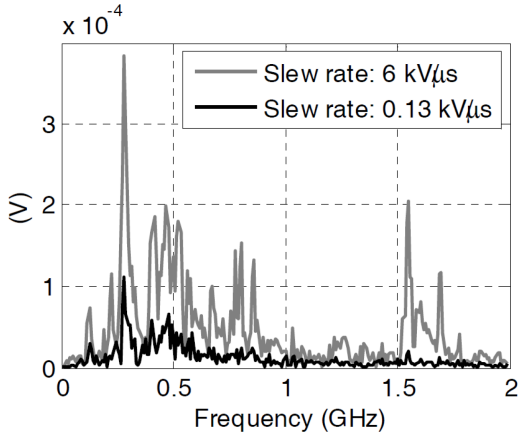

Fig. 11. Effect of rise time on PD pulse spectra [36].

voltages with a peak voltage equivalent to a 50 Hz sinusoidal voltage.

Upon observation, when the rise time is 150 ns, voltage overshoot is observed, and there is no difference in evaluating the PDIV using either the peak voltage or the DC bus voltage. However, for rise times of 7 to 15 ns, the overvoltage is more pronounced. In the case of fast-rising voltage pulses, higher PDIV values result from the negligible probability of initiating an electron when the waveform reaches the inception level. As the probability becomes significant, the voltage rises rapidly, leading to larger PDIV recordings. Therefore, according to [43] the peak value is a good estimator for the PDIV when the overshoot is negligible.

In agreement with [42] and [43], the research carried out by [36] regarding the influence of rise time on the PD phenomenon indicates that no substantial correlation exists between the PDIV or RPDIV and rise time. Nevertheless, it is worth noting that this parameter can exert an influence on the PD pulse spectra. As shown in Fig. 11, it is clear that a sharper or faster pulse (pulse with a higher *dv/dt*) produces higher frequency content within the PD pulse spectra.

In the ongoing investigation into the effect of rise time on PD patterns and considering the superior switching capability of SiC devices compared to Si devices, [44] analysis the PD pattern under three rise time conditions (100, 120, and 150 ns), simulating the voltage pulses generated by SiC devices, along with a 1000 ns rise time generated using a Si-based voltage generator. In this study, to mitigate the effect of charge accumulation, during each test step, a single pulse voltage is applied to the test sample. As per the findings in [44], a decrease in rise time results in a reduced PDIV. This observation is elucidated by the earlier initiation of initial electron generation in voltage pulses with a faster rise time.

PD tests conducted with varying rise times and pulse widths demonstrated a reduction in PDIV by up to 38% when transitioning from a 1000 ns rise time generated by a Si IGBT to a 100 ns SiC MOSFET. In this study, PD samples consist of twisted pairs, and detection is carried out using a high-frequency current transformer and a PMT. The obtained results contradict

the analyses and test outcomes of [34], [40]. While [44] attributes the differences to variations in applied excitation and test procedures, especially the use of a single-pulse voltage for PD tests, [40] employs a similar technique but reports contrasting observations.

The impact of rise time on PDIV has been a topic of study in the literature, leading to diverse and contradictory findings. Some researchers have reported that increasing rise times result in higher PDIV values, while others have observed the opposite trend with decreasing PDIV values or no variation.

The discrepancies in reported findings regarding the effect of rise time on PDIV values can be attributed to inconsistencies in terms of sample material properties, environmental conditions (such as humidity and temperature) surrounding the test setup, and applied voltage waveforms–whether using a single pulse test or applying continuous pulse voltages, which may impact the result through space charge accumulation.

Another influential factor is the testing procedure employed for the PD test. For instance, incorporating resistors in series with the test sample as a safety measure to regulate current in the event of sample breakdown has been adopted. The series resistor R forms an RC circuit with the test specimen's capacitance C. As a result, the voltage across the specimen rises with a time constant RC rather than following the actual *dv/dt* of the waveform generator or motor drive. This aspect is particularly crucial in WBG-based drive studies, where the primary objective, as mentioned in the literature, is to analyze the impact of fast and ultra-fast rising pulses. Further more addition of the R may impact the low impedance PD events. Despite these considerations, there is currently a lack of comprehensive analysis regarding the effects of implementing protective measures on PD test results.

B. Frequency

The PWM voltage output generated by motor drives comprises a fundamental component at a low frequency and additional harmonics at the high-frequency switching rate. As a result, a detailed examination of how frequency affects PD phenomena becomes crucial. To address this, multiple studies have been conducted, focusing on investigating the influence of pulse frequency on key PD characteristics, including PDIV and RPDIV. This research pursuit of understanding frequency's role is further motivated by the potential advantages associated with the utilization of SiC devices, which can extend the achievable operational frequency range. Similar to the investigation of rise time effects mentioned earlier, the exploration of how PWM voltage frequency impacts the scenario has also yielded diverse insights within the existing body of literature.

In the realm of studies investigating the impact of PWM characteristics on PD behavior, [36] notably examines the influence of frequency on PD patterns. Using crossed wires as the experimental sample and accompanied by a pulse voltage generator, the setup is designed to generate voltage pulses with a consistent duty cycle and rise time while allowing for variable frequency. Consequently, increasing the pulse frequency corresponds to a decrease in the duration of voltage application across the sample and voltage cancellation or zero-volt duration within each cycle.

To capture RPDIV, which entails observing at least 5 PD events in every ten pulses, the residual space charge lingering from preceding PD occurrences is pivotal in facilitating subsequent PD phenomena. This residual space charge also augments the electric field intensity within the PD area at the moment of polarity reversal. In [36] postulates that due to these twin mechanisms, each PD event's presence can catalyze subsequent events' occurrence.

Conversely, during the cycle's zero-volt duration, the impact of the residual space charge diminishes as charges migrate into traps. Hence, the zero-volt duration of the cycle can be termed the "charge decay duration." As a result, a shorter zero-volt duration within the cycle indicates a diminished presence of space charge. Succinctly, reducing the zero-volt duration enhances the probability of PD events during the voltage application time in each cycle. This suggests that decreasing the zero-volt interval can increase the likelihood of PD events during the voltage application. Consequently, an increase in frequency correlates with a reduction in RPDIV, as elucidated by [36]. However, this study does not provide insight into the effect of frequency on PDIV value.

Consistent with the findings of [36], the results from studies conducted by [45] on the impact of frequency on PD patterns, utilizing twisted wires as PD test samples and a SiC-based pulse generator capable of switching up to 200 kHz, indicate that the RPDIV decreases with increasing frequency. However, it reaches a plateau for frequencies higher than 100 kHz to 200 kHz. The higher RPDIV observed for frequencies lower than 100 kHz is attributed to sufficient time for charge relaxation. Nevertheless, the saturation behavior of RPDIV beyond 100 kHz lacks a clear justification. Interestingly, repeating the same tests under lower air pressures has demonstrated a similar pattern. It's worth noting that the influence of ambient conditions on PD patterns is beyond the scope of this paper.

On a different note, another study, [46], argues that the influence of frequency on PDIV value is minimal. Their investigation involving twisted wire samples reveals that raising the frequency from 1 kHz to 5 kHz results in only a slight PDIV elevation, roughly 6%.

In an examination of a high switching frequency capable setup, as investigated by [15], PD tests were conducted by sweeping the test frequency, generated by a SiC-based inverter, from 10 to 100 kHz. The study maintained a fixed rise time of 8 ns and compared the results with PD tests conducted under a 50 Hz sinusoidal voltage. In agreement with [46], the findings indicate that PDIV is not dependent on the switching frequency. Further insights into this conducted study are detailed in [43], which attributes the observed discrepancy between the findings of [15], [43] and those of other literature regarding the dependency of PDIV value on frequency to significant dielectric losses in the tested wires at the selected specific test frequencies.

In a further exploration of the impact of frequency on PDIV and RPDIV, [47] conducted experiments to measure both parameters in a twisted pair sample excited with a SiC-based pulse generator through a PMT. The study ensured a consistent pulse width of 500 ns for all tests, aiming to eliminate the duration effect of voltage application. A fixed rise time of 23 ns was chosen to guarantee an

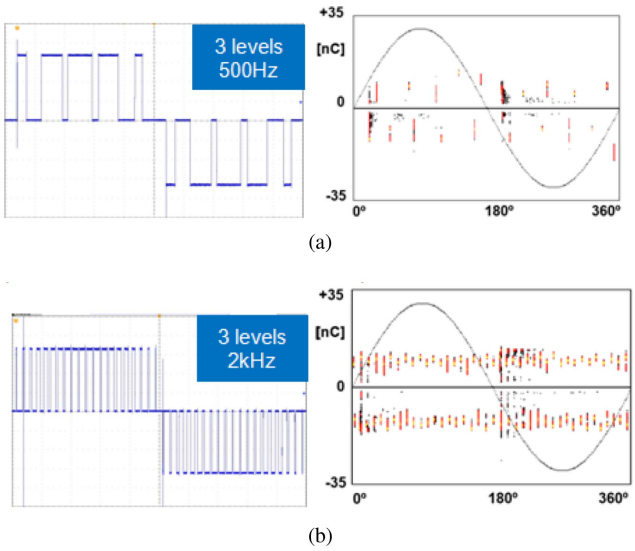

Fig. 12. PD patterns corresponding to a 3-level voltage waveform with (a) 500 Hz and (b) 2 kHz switching frequency.

overshoot-free voltage waveform, thereby preventing the impact of instantaneous voltage on studies analyzing the effect of dv/dt on PD patterns, a solution similar to [48].

The test results, obtained by varying the pulse repetition frequency (PRF) from 60 pulses per second (pps) to 1 Mpps, revealed that PDIV is not dependent on the frequency. However, RPDIV exhibited a significant frequency dependence. This observed dependency can be attributed to two main factors. Firstly, an increase in temperature occurs with the rise in frequency, which reduces the PDIV. Secondly, increasing the switching frequency while keeping the pulse width similar reduces the charge decay time, which reduces RPDIV. Measurements of the sample's temperature after high-frequency tests showed a negligible difference, which supports the second justification [47].

Moreover, studying the PD magnitudes and delay time defined as the time between the zero crossing time of the square wave voltage and the occurrence of the PD event, with increasing the test voltage frequency from 2 Hz to 5 kHz, repetition rate of PD events, their average magnitude and delay time decrease [49]. Using the surface charge analysis, [49] concludes that increasing the supply voltage frequency decreases the surface discharge decay ratio between two subsequent discharge events. Therefore, because of the electric field induced by surface charge, which strengthens the background electric field, applying a lower electric field can generate PD events.

Furthermore, based on the Richardson-Schottkey emission law, the emission probability of free electrons increases because of a lower surface charge decay ratio. In high frequencies, observing PD events in a lower electric field, produced from a lower voltage level, justifies the lower PD amplitudes and higher possibility of providing the first free electron, which explains the lower delay time for achieving the PD events in higher frequencies.

Similarly, the impact of frequency on PD magnitude is also tested in [50]. According to results (Fig. 12), higher switching frequency increases the PD magnitude. Further, it can be observed that switching frequency can affect PD lag, which can be defined as the time after the voltage step and the time PD activity initiates. Based on the test results, a higher number of severe PD events can occur at lower switching frequencies on the pulse plateau of the modulating voltage. While multiple studies, including [51], have demonstrated that PD activities often manifest in the rising and falling flanks of the voltage waveform.

C. Impulse Width (Duty Cycle)

The influence of the duty cycle in PWM voltages or square-wave voltages has also been investigated in the literature. However, it is generally considered less significant than factors like rise time and switching frequency, primarily due to the difficulty of directly controlling the duty cycle in practical applications that utilize PWM techniques. Consequently, a relatively restricted number of publications have explored the impact of the duty cycle.

To assess the influence of impulse width, or duty cycle, on PD, [36] employs crossed wires as a test sample, simulating motor windings, a variable duty cycle voltage generator, and a horn antenna for PD detection. The impact of increasing impulse width on the PDIV and RPDIV is presented in Fig. 14, revealing that while the PDIV remains unaffected, the RPDIV experiences a significant reduction. This observation finds justification in the distinct nature of PDIV and RPDIV. Indeed, PDIV can be acquired when the voltage level is high enough and an initiating electron is present. Therefore, PDIV should be independent of impulse duration if the voltage increases slowly enough. Conversely, the definition of RPDIV necessitates the observation of at least five PD events within every ten pulses, implying that the likelihood of PD occurrence in each cycle must exceed 50%. The pivotal point to underscore here is that deposited electrons, generated after each PD event, can increase the probability of initiating the subsequent PD events, particularly when the electric field achieves a significant intensity [36].

To explain the variation of RPDIV with duty cycle, [36] uses the Schottky-Richardson emission model. This model is represented as follows:

$$\frac{dn(t)}{dt} = n(t)v_0\, exp\left(-\frac{\Psi - \sqrt{\frac{q_e|E|}{(4\pi\varepsilon_0)}}}{KT}\right)$$

Where $\frac{dn(t)}{dt}$ is the number of electrons emitted per unit of time from the surface of the twisted pair in the area where the electric field is high enough to initiate an avalanche and $n(t)$ is the number of the available electrons at the same region. v_0 is the the fundamental phonon escape frequency, Ψ the height of the emission barrier, E is the electric field at the twisted pair surface, K is the Boltzmann constant and T is the temperature.

According to the Schottky-Richardson model, a higher electric field, which is generated with an elevated voltage level, results in the production of more free electrons within each time unit. In simpler terms, this implies a reduced time interval between reaching the PDIV level and the occurrence of PD

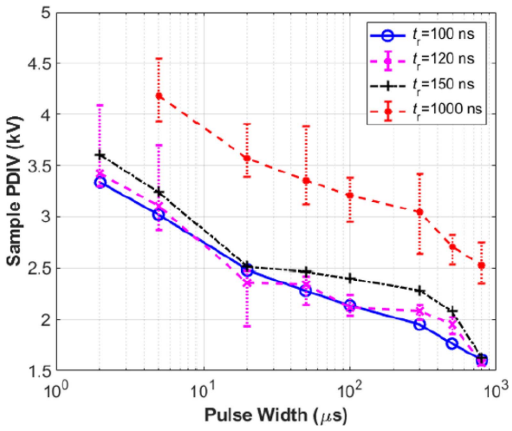

Fig. 13. PDIV results versus pulse width under various rise times [44].

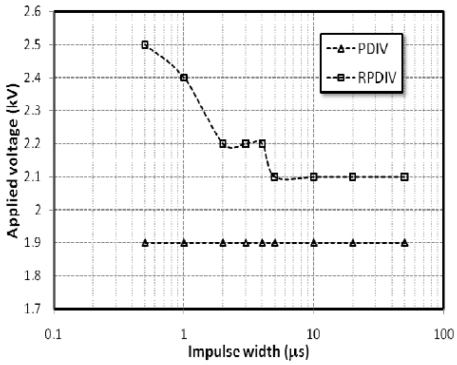

Fig. 14. Impact of impulse width on PDIV and RPDIV [36].

events. When the pulse width is shorter than this delay period, subsequent PD events might not manifest as the voltage stress diminishes before PDs can arise. Conversely, if the pulse duration is sufficiently extended, even at lower voltage levels, it becomes possible to record the RPDIV after reaching the PDIV level. Consequently, for narrower impulse widths, or pulses with lower duty cycle, a higher applied voltage is required to achieve the RPDIV level [36].

Contrary to the conclusions drawn in [36] regarding the impact of pulse width on the PDIV value, [44] asserts that an increase in pulse width actually diminishes the PDIV value. This observation is rationalized by the concept of initial electron generation. In the case of a pulse with an extended width, given a constant rise time, the initiation of initial electrons can occur over a more prolonged duration, as long as the applied voltage surpasses the threshold. Consequently, a lower voltage level would be adequate to initiate the PD. Results of this study is depicted in Fig. 13.

In the examination of the impact of pulse width on PDIV, as discussed in [44], the PD tests involve the application of a single pulse to a twisted pair. Consequently, the study does not account for the effects of voltage cancellation duration present in a period.

In contrast, [52] offers a distinct perspective based on their PD tests using a twisted pair of wires. Taking into consideration the

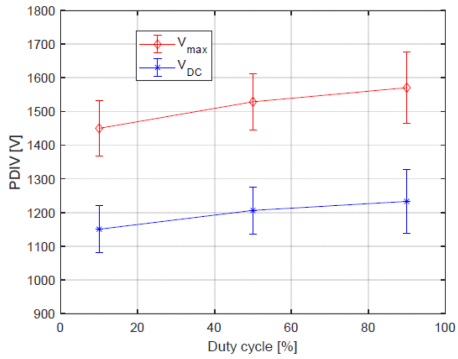

Fig. 15. Impact of duty cycle on the PDIV, switching frequency fs = 100 Hz, rise time = 70 ns. [52].

influence of voltage cancellation time, this study emphasizes the duty cycle as a potential factor affecting PDIV instead of pulse width. The findings suggest a substantial impact of the duty cycle on the PDIV value. In this reference, a unipolar square wave is employed for their PD tests, and PD events are detected using a coaxial cable sensor. The results, illustrated in Fig. 15, show that an increase in the duty cycle corresponds to a rise in PDIV. Notably, the frequency and rise time are maintained constant throughout the tests to isolate the effect of other factors. Additionally, by keeping the rise time fixed, the voltage amplitude considering the overvoltage (Vmax) maintains a consistent ratio, approximately 1.26, to the applied supply voltage (VDC).

In [52] rationalizes the observed relationship between duty cycle and PDIV by the shorter time available for charge redistribution during the voltage cancellation interval, or the non-conducting period, within pulses characterized by a higher duty cycle.

Furthermore, the behavior of PD within rising and falling flanks of pulses with varying duty cycles is investigated in [37]. The study reveals that a 50% duty cycle yields a symmetrical PD pattern, whereas a shorter positive impulse width results in PD events of diminished magnitude during falling flanks, as illustrated in Fig. 16. It is essential to emphasize that the applied voltage in tests performed in this research is a bipolar voltage oscillating at 10 kHz frequency, encompassing transitions from positive to negative voltage and vice versa. It's notable that in this reference, the duty cycle is described based on the duration of the positive impulse within a cycle.

In addition to investigating the correlation between the magnitude of PD events and the duty cycle, [37] also delves into the repetition rate of PD occurrences during both the rising and falling edges of impulses. In this context, the reference defines the PD repetition rate as the average count of PD events aligned with the rising and falling flanks. Fig. 17 illustrates that the repetition rate of PD events during rising flanks hovers around one, implying that each transition from negative to positive voltage triggers a PD event. Conversely, for falling flanks, the PD repetition rate hinges on the duration of the positive impulse voltage. It is noteworthy that throughout the alterations in positive impulse length, the cycle time remains consistently set at 100μs. Therefore, this study asserts that the duration of the

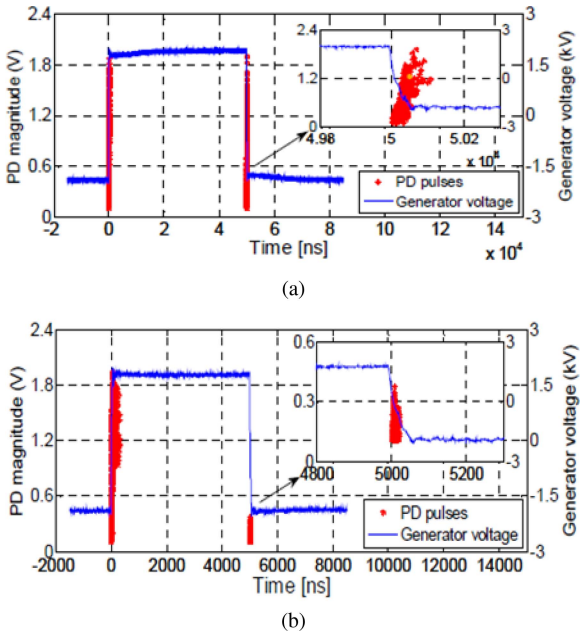

Fig. 16. Effect of duty cycle on PD magnitude, (a) 50% duty cycle (b) 5% duty cycle [37].

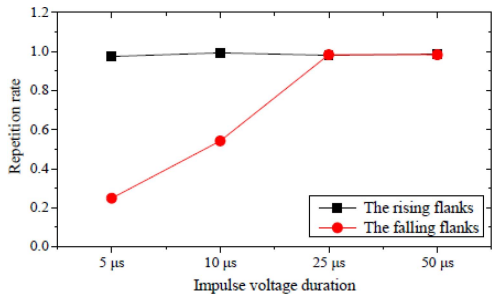

Fig. 17. Effect of impulse voltage duration on repetition rate of PD for positive and negative voltage flanks [37].

pulse can influence the number and magnitude of the PD events, which is aligned with the findings of [52] and [53] in establishing a correlation between the behavior of PD and variations in the duty cycle.

D. Voltage Waveform Shape

The increasing adoption of VSDs has enabled higher power density and improved control over motors. However, it is crucial to consider the inherent waveform of the output pulse-width modulation (PWM) voltage from these drives, as it could potentially have a negative impact on insulation durability [54].

In investigating the effect of voltage waveform shape or the number of voltage levels generated by motor drives on PD patterns, comprehensive tests have been conducted and documented by [55]. These experiments encompass sinusoidal voltage supplies and two-level, three-level, and five-level inverters applied to twisted pair as the test samples for PD testing (refer to Fig. 18). The key finding is that increasing the number of voltage levels

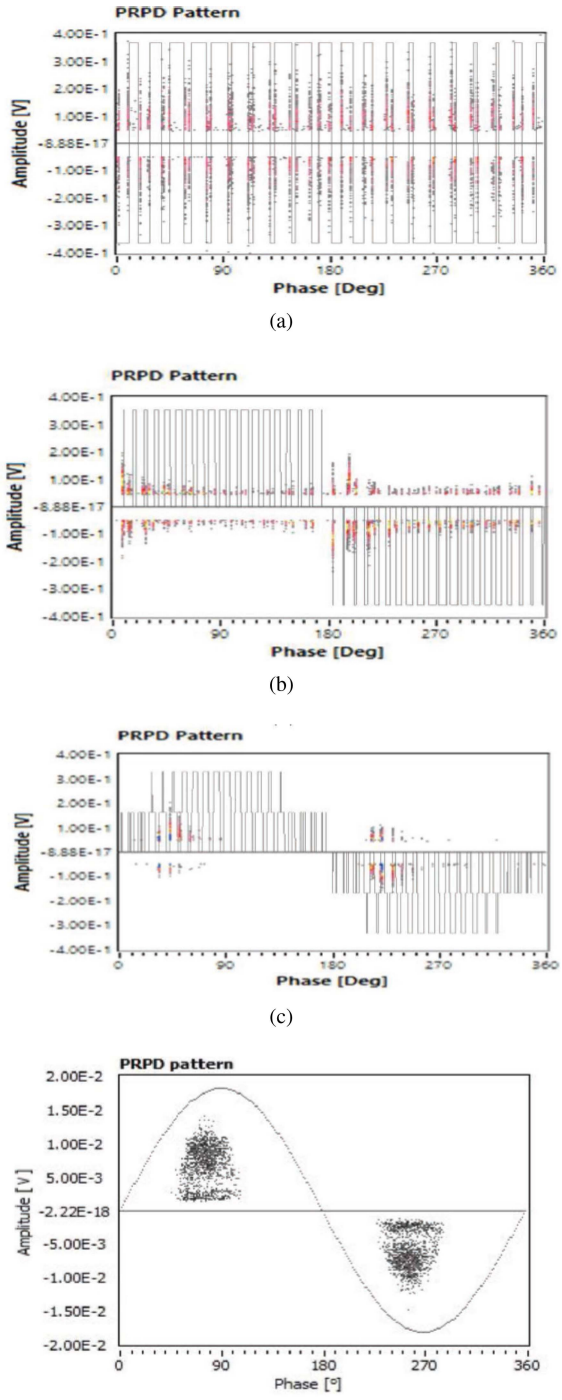

Fig. 18. Effect of number of voltage level on PD pattern (a) Two level, (b) Three level, (c) Five level, (d) Sinusoidal [55].

reduces PD magnitude and brings the PD pattern closer to that observed with a sinusoidal voltage source [55].

A similar study is performed by [50], and the employed test setup is depicted in Fig. 19. As shown in the test setup, for generating multi-level voltages, an inverter stage containing four Full-Bridge inverters, noted with FB cell on Fig. 19, is used. This unit is capable of generating up to the nine-level voltage waveform. The PD activities in this setup are detected using a

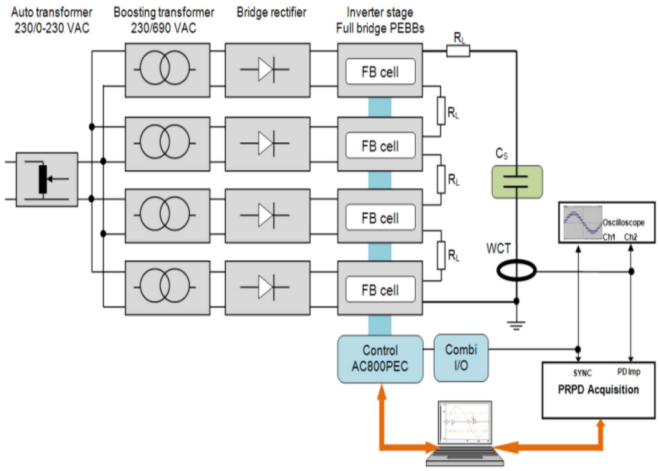

Fig. 19. Modular multilevel converter topology and PD measurment setup [50].

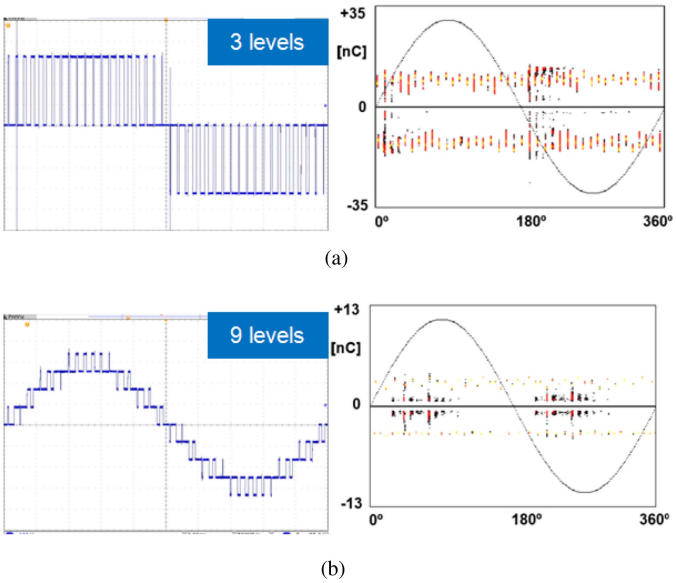

Fig. 20. Voltage waveforms and corresponding phase resolved patterns (a) Three-level, (b) Nine-level [50].

TABLE III
PD MAGNITUDE VERSUS NUMBER OF VOLTAGE WAVEFORM LEVEL [50]

Number of voltage level	PD magnitude (nC)
3	11.3
5	5.1
9	3.1

galvanically isolated high-frequency current transformer, with the test sample denoted as "Cs" representing the twisted pair specimen. Waveforms for three-level and nine-level voltages, as well as the phase-resolved PD patterns for each voltage waveform, are showcased in Fig. 20. It can be observed that with increasing the voltage waveform level, the density and intensity of the PD events decrease dramatically. Table III demonstrates the PD magnitude for voltages with different numbers of levels. This observation underscores the correlation between the magnitude of PD and the size of fragmented step changes in voltage, indicating that more minor step changes result in correspondingly smaller PD magnitudes. In [50] attributes this observation to prompted discharge initiation due to the higher electric field in the discharge area generated by higher step voltage variation of the voltages with a lower number of levels.

In alignment with the findings of [50] and [55], [56] affirms that the decreased voltage step change observed in a three-level inverter, in comparison to a two-level inverter, results in a reduction in PD density. Furthermore, the study emphasizes that, beyond the voltage level's significant impact on the PD pattern, distinct types of PWM voltage waveforms, unipolar and bipolar, manifest differing PD behaviors. Within the context of two-level inverters, the voltage step change associated with unipolar voltage waveforms is half that of bipolar PWM voltage waveforms. This discrepancy leads to a diminished density of PD events for unipolar PWM configurations.

E. Deadtime

Deadtime refers to the delay between gating signals of switching devices within a phase leg, implemented to prevent current shoot-through during switching transitions [57], [58]. In motor drives designed to operate motors, incorporating deadtime into PWM switching signals serves the purpose of safeguarding the switching devices. However, this protective measure comes at a cost, as it leads to a decrease in motor insulation lifetime due to the generation of current harmonics and additional losses [59], [60], [61].

Recognizing the significance of these concerns, a study conducted by [62] delved into analyzing the influence of deadtime on the pattern of PD, which stands as one of the most pivotal factors contributing to insulation degradation. This investigation employed enameled crossed wires as PD test samples and utilized a UHF antenna to detect PD events. The study focused exclusively on the deadtime between switching devices as the variable of interest, while keeping the peak-to-peak bipolar test voltage, rise time, and switching frequency at constant values. The bipolar test voltage is generated by a full bridge inverter configuration comprising high voltage switches and real-time control hardware [63]. Notably, the voltage across the sample reaches 0 V during the deadtime interval.

The study encompassed testing with varying deadtime values, ranging from 0 to 10 μs, leading to the observation that the intensity of PDs post-deadtime is significantly higher than the conditions prior to the deadtime, for both the rising and falling flanks. Additionally, Fig. 21 showcases the manifestation of PD events both before and after the deadtime for both raising and falling flanks and further insights into the distribution of PD events before and after a 2 μs deadtime, during the rising and falling edges of the square wave voltage, are presented in Fig. 21.

The investigation demonstrates that increasing the deadtime significantly impacts the quantity of PD events. Fig. 22 succinctly summarizes this variation, where the first rising time corresponds to the rising flank prior to deadtime, and the second rising time relates to the rising flank post-deadtime. Similarly,

TABLE IV
IMPACT OF PWM CHARACTERISTICS ON PD

PWM Characteristic	Ref.	Summary of Impact on PD Pattern
Rise time	[34] , [39], [40]	Increasing rise time decreases the PD magnitude and PD firing voltage.
	[44]	Increasing rise time increases the PDIV.
	[40], [67]	Increasing rise time decreases number of PD events, and highest PD magnitude in each cycle.
	[15], [36], [42], [43], [64]	Rise time does not affect PDIV.
	[42]	Faster rise time generates PD pulses with higher frequency content.
Frequency	[36], [45], [47]	Increasing frequency reduces RPDIV.
	[15], [43], [46] , [47]	Frequency does not severely affect PDIV
	[49], [39]	Increasing frequency reduces PD magnitude, repetition rate and delay time .
	[50]	Increasing frequency increases PD magnitude and lag time.
	[67]	High frequencies increase PD events but decrease individual PD intensity.
	[51]	High frequencies give rise to PD events to appear near to flanks
Pulse width (Duty cycle)	[36]	Increasing pulse width does not impact PDIV but decreases RPDIV
	[44]	Increasing pulse width decreases the PDIV
	[52]	Increasing duty cycle slightly increases the PDIV
	[37], [53]	For a bipolar pulse voltage, increasing the impulse duration increases the PD repetition rate and magnitude.
Voltage shape	[50], [55], [56], [68]	Increasing voltage level, decreases magnitude of PD events.
	[56], [68]	Bipolar PWM voltage gives rise to more intensive PD events than unipolar PWM.
Deadtime	[62]	Increasing the deadtime increases the total number of PD events and accelerates aging.

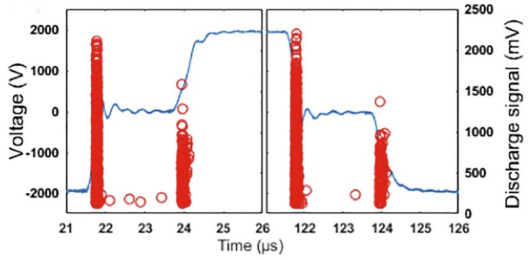

Fig. 21. PD distribution before and after 2 μs deadtime for rising and falling flanks [62].

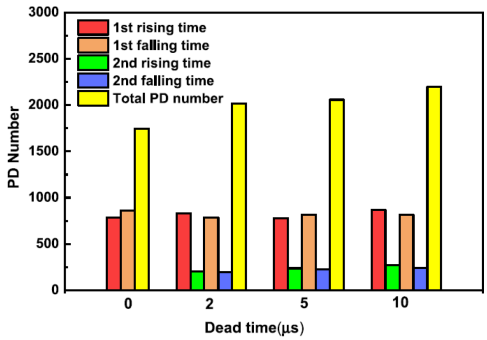

Fig. 22. PD distribution summary for various deadtime values [62].

the first and second falling times correspond to falling flanks before and after the deadtime, respectively. Two key observations can be drawn from Fig. 22. Firstly, incorporating deadtime substantially increases the number of PD events, as compared to the scenario without deadtime (0 μs deadtime). Secondly, following the introduction of deadtime, the number of PD events during the first rising and falling times surpasses those during the second rising and falling times. This phenomenon can be attributed to the polarity reversal of the electric field established before the deadtime, triggered by overvoltages. At the onset of the first rising and falling edges, the generated electric field aligns with the electric field stemming from surface charges, potentially exceeding the critical electric field and inducing PD events. Conversely, the electric field generated during the second rising and falling edges opposes the surface charge electric field, reducing the likelihood of PD occurrence. The lower amplitude of the discharge signal depicted in Fig. 21 further corroborates this rationale [62].

As discussed in this section, the literature highlights that various aspects of the PWM voltage generated by motor drives can potentially influence the PD pattern and contribute to insulation aging. However, differing opinions, especially regarding features like rise time and frequency, exist on how they specifically impact PD. Table IV summarizes various references' perspectives on the influence of each PWM characteristic on the PD pattern.

The observed variations in the literature reported results can be attributed to differences in test approaches, including voltage application methods, PD detection systems, sample preparation procedures before testing, and environmental conditions in the test area. To address and reconcile disagreements in the results, rather than solely focusing on maintaining consistent environmental conditions, three alternative considerations can be particularly helpful.

Firstly, It is crucial for researchers to determine the insulation type of their samples. If the insulation is organic, it falls into the Type I category, and, as per [18], using twisted wires is acceptable for testing turn-to-turn insulation. In the case of PD-resistant material in the insulation system, selection of PD test samples should align with [20]. For Type II insulation material, which encompasses PD-resistant material, [20] mandates the use of a motorette or complete winding for turn-to-turn insulation tests, particularly in motors with random wound winding.

Given the significance of adhering to the appropriate standards based on the insulation material, questions may arise regarding the accuracy of results reported in research such as [64], where twisted wire samples are employed for PD testing on wires with both Type I and Type II insulation material.

Another significant consideration is the impact of different test procedures on results, potentially leading to misguidance and errors in insulation system assessment. For example, when

assessing the effect of rise time on the PD pattern, some literature employs a single pulse to mitigate the effect of charge accumulation, such as [44], while others, following the approach in [26], use a specific number of pulses, such as [47], and some maintain continuous testing during PDIV measurement.

Lastly, variations in test setups, such as the use of a tens of $k\Omega$ resistor in series with specimens for protection in case of sample breakdown, as seen in [44], [50], [65], [66], raise concerns. The lack of guidance on selecting the appropriate resistor value is noted. Using a large resistor can hinder low-impedance events by impacting the charge accumulation process, and potentially skewing results. Consequently, to ensure consistency in studies, results, and analyses, specific guidelines are crucial to standardize test procedures.

IV. PD Detection Methods

The PD detection involves measuring the intensity and localizing the discharge [69], [70]. The intensity of the charge is normally measured in nQ. Localization is based on finding the location where the intensity of physical phenomenon associated with PD events is maximum. For PD detection in motors, two approaches exist offline and online testing. In offline testing, the motor is taken out of service, and a separate test power source is employed to energize the winding for PD detection. On the other hand, in online testing, the rotating machine is operated normally and is connected to the power source.

The standards IEC 60034-27-1 and 60034-27-2 provide guidelines for PD detection in motor windings for offline and online testing, respectively [71], [72]. IEC 60034-27-1, based on the offline portion of IEEE 1434, emphasizes the use of capacitive-coupled units. In contrast, IEC 60034-27-2 also permits the use of High-Frequency Current Transformers (HFCT) and microwave antennas in addition to capacitive couplers. This is because online testing introduces more noise, including harmonics and disturbances from the running motor, especially in the Low Frequency (LF) range ($<$ 1 MHz), where the output from the capacitive coupler is more susceptible to getting corrupted or hidden under the noise [73]. HFCTs and antennas aid in capturing the PD signal in the High (3-30 MHz), Very High (30-300 MHz), and Ultra High (300-3000 MHz) Frequency (HF, VHF, and UHF) ranges, where the PD signal has a higher Signal-to-Noise Ratio (SNR), reducing the risk of false positives. A High Pass Filter (HPF) is used to filter out the LF power harmonic noise to augment measurement accuracy. Nevertheless, as the frequency increases, the range of PD detection and localization is reduced due to high attenuation at higher acquisition frequencies. Further, it is pertinent to mention that these standards apply exclusively to motors powered by an AC source, not VS-PWM motor drives.

Detecting PD in motors powered by VS-PWM motor drives proves more challenging than those powered by AC sources. The primary challenge arises from the switching action inherent in VS-PWM motor drives, generating a broad spectrum of electromagnetic interference extending up to VHF range [74], [75]. Consequently, the switching noise makes the PD signal susceptible to being overshadowed, posing difficulties in its detection and differentiation [76]. The challenges are further exacerbated with the increased adoption of WBG devices for motor drives, owing to their high dv/dt switching capability (Fig. 1).

To address these challenges, the IEC 60034-27-5 standard, based on IEC 60034-27-1, 61934:2011 and 62748, provides guidelines for offline PD detection in stator windings powered by VS-PWM drives [77]. This standard has been adopted in recent works investigating PD in motors powered by VS-PWM drives [32], [75], [78]. In contrast to the IEC 60034-27-1 offline standard designed for motors powered by AC sources up to 400 Hz, this standard also suggests using HFCTs and electromagnetic couplers in addition to capacitive couplers to augment PD detection in PWM noise environment. Moreover, the standard specifies using high-order HPF filters to effectively filter out the drive-switching noise.

Besides IEC 60034-27-5, another emerging method for PD detection in motors fed by VS-PWM drives includes "Blackout Testing" with ultraviolet (UV)-sensitive imaging devices, initially proposed in the IEEE 1799 standard for motors with rated line-to-line voltage greater than 2300 V at power frequency [79]. This method captures the optical signal or light emitted during PD events in a spectral range from infrared to ultraviolet (280 nm to 405 nm) [80].

The following subsections review the detection methods and practises employed in the literature.

A. Coupling Capacitor

The coupling capacitor is the classic method employed predominantly in online PD detection in motors fed with an AC source. The PD is measured using a capacitor connected to the motor stator winding terminal on one side and a 50 Ω resistor on the other. The capacitor and resistor form an HPF and the cutoff frequency is set to a low frequency around 1 MHz [71], [72]. The capacitor impedance is high for AC power frequency, and hence, the capacitor blocks power line frequency components. On the other hand, PD has a rise time in ns, with spectral content reaching several hundred MHz. Therefore, the PD pulse passes through the coupling capacitor and the 50 Ω resistor, producing voltage as a signature that can be used to detect PD and estimate charge.

In the context of VS-PWM drives, the coupling capacitor approach introduces a challenge involving significant interference from PWM switching transients. These transients lead to impulses in the detector output, reaching magnitudes in the order of tens of volts [81]. Consequently, the PD signal is overshadowed, leading to erroneous detection unless a filter and a stable AC voltage reference are provided. Additionally, this method lacks the capability for localization, and the range of PD detection is contingent upon the winding structure. If the PD originates far from the capacitor, its propagation through the winding may be severely attenuated, rendering it undetectable.

In the literature, the adoption of this method for VS-PWM drive-fed motors is limited, with few examples centered on online PD detection in Si-based drives. For instance, in [82], the method is implemented for online PD detection in a high-voltage motor powered by a Si-based VS-PWM drive for the oil industry. Challenges related to filtering interference from PWM switching transients and noisy AC references are addressed, and solutions

are proposed. Further, it is pertinent to note that, in literature, this method is overlooked for PD investigation in twisted wires and stator coils with PWM excitation. This oversight may be attributed to its non-isolation and the need for a physical, electrical connection with the test specimen, coupled with its perceived inferior performance in handling fast switching transients and distinguishing PD [73], [81]. This is especially notable compared to alternative approaches, like electrocouplers, HFCTs and PMT, particularly with the transition from Si to WBG devices.

B. Electromagnetic Couplers

Among the methods specified in IEC 60034-27-5, electromagnetic couplers, being non-invasive, are popular, extensively researched, and employed for detecting PD in twisted pairs or stator windings with PWM excitation. The most common type of electromagnetic coupler used is the UHF antenna, which is placed near the test specimen to capture the far field of the PD event in the UHF range. This measurement technique is highly localized, and sensitivity depends on the distance from the PD source in the specimen and the type and shape of the antenna.

Generally, one UHF antenna is used for twisted pairs, as the objective is to detect PD activity with high sensitivity [15], [32], [43], [83], [84], [85], [86]. In contrast, for the full stator winding and online PD testing, it is essential to localize the PD source. For this purpose, the general practice is to place multiple UHF antennas around the stator winding or motor. For instance, in [87], a patch antenna array is designed for the bare stator core to maximize PD reception and localization. Likewise, in [88], a shell slot antenna for online testing is developed where the existing multiple slits on the motor housing are employed as a UHF antenna without installing any specific sensors or couplers externally. The efficacy of the antenna is validated using both twisted pairs housed inside the shell for turn-to-turn, and winding for phase-to-ground PD tests. For benchmarking, an Archimedes Spiral Antenna (ASA) is also used. According to the test results, the shell slot antenna gives consistent output as ASA for phase-to-ground PD while exhibiting slightly lower sensitivity for turn-to-turn PDs.

Besides far-field, UHF near-field electromagnetic couplers are also employed for PD detection. These couplers are based on capacitive (E-field) or inductive (H-field) coupling. They are placed in proximity (near-field) to the windings terminals or cables. In [89], a disk-shaped loop antenna array is developed and placed 2 cm away from the stator coil end of the actual motor. The antennas capture the near H-field emissions from the PD, and the network of these antennas aids in localization.

Similarly, in [90], a combination of E-field couplers, including D-dot antenna, stripped coaxial cable, and Jack-SMA connector, are benchmarked for PD detection in a PWM environment using twisted pair as a sample. According to the results, the performance of low-cost stripped coaxial cable is comparable to that of the commercially available D-dot sensor. Further, in [74], a cable-mounted Jack-SMA-based capacitive electromagnetic coupler is devised to detect PD in motors for aircraft applications. The approach is similar to conductive capacitive couplers, except that the sensor is not phsically connected to the cable conductor. Although the sensor is effective and safer due to its non-invasive nature, it requires the power cable shield to be removed to maximize coupling.

While UHF-based near and far-field couplers prove effective for PD localization with an extensive measurement range, there are numerous challenges associated with their data acquisition. Firstly, the output of these couplers contains the PWM switching spectral content in LF, HF and VHF ranges, which needs to be filtered. For this purpose, IEC 60034-27-5 specifies the use of an analogue high-order HPF. However, with WBG devices that can reach high slew rates upto 50 V/ns (Fig. 1), the switching noise spectrum can spread far in the UHF range, overlapping with the PD spectrum. Besides this, the PD spectrum is also attenuated significantly with high-order, making small PDs undetected. Secondly, the filters do not necessarily provide a linear phase throughout the frequency range, leading to a time shift in the output. This can lead to the false alignment of PD event with the excitation voltage in the time domain [86].

Lastly, due to their UHF measurement range, electromagnetic couplers require oscilloscopes with high sampling rates, which are expensive. To address this limitation, a frequency downmixing approach has recently been proposed and adopted in [83], [91]. In this method, the PD signal with frequency f_1 in the UHF range is mixed with a single high-frequency sinusoid with frequency f_2. A down mixer and a low-pass filter are employed to extract the low-frequency shifted component $|f_1 - f_2|$, which can be easily detected using a low-bandwidth measurement system.

C. HFCT

HFCT is another non-invasive method listed in IEC 60034-27-5 for PD detection. The transformer is placed in the line; therefore, this method does not allow PD localization. HFCTs have been extensively used in recent studies for PD detection in motor windings with PWM voltage excitation [76], [92], [93]. However, there are some challenges associated with the HFCT method.

Firstly, the HFCT is placed in the line, which is contaminated with switching transient currents. Detection of PD during fast switching edges is cumbersome due to the possible overshadowing of the PD signal by the switching noise [76]. Secondly, as with electromagnetic couplers, a high-pass filter (HPF) with a proper cut-off frequency and linear phase response is required to filter out unwanted noise. Lastly, as for the capacitive coupling technique, the sensitivity of HFCT for PD detection depends on the specimen's structure and impedance response. Complete stator windings are both capacitive and inductive. A PD pulse originating deep inside the winding has to travel across the complex impedance network with a higher tendency to get attenuated significantly before being sensed by HFCT. For this purpose, a common practice adopted in literature for PD detection under a PWM environment is to use a UHF antenna in conjunction with HFCT [86], [91], [93], [94].

Moreover, the accuracy of the detection method relies on the bandwidth and sensitivity of HFCT. For achieving high bandwidth, HFCTs are built using ferromagnetic cores such as Manganese and Zinc (MnZn) [92]. Nonetheless, using ferromagnetic material leads to nonlinearity in the transfer function.

The nonlinearity is dependent on frequency, temperature, and flux density. The temperature dependence concerns the accurate estimation of PD intensity in windings of motors for aircraft applications operating at lower or cryogenic temperatures unless a comprehensive characterization of HFCT at those temperatures is available. For addressing the transfer function nonlinearity, a Rogowski Coil-based HFCT approach without a ferromagnetic core has been proposed recently in [95], which provides a linear transfer function. However, the bandwidth of the Rogowski coil prototype is limited to 10 MHz, restricting its usage within HF range.

D. Optical/UV Detection

In recent years, there has been a surge in the use of optical methods for detecting PD, especially in studies that examine the effects of high dv/dt in SiC devices [15], [32], [44], [83], [86]. This method involves detecting the light or optical signal emitted by the PD using PMT or photon counters [79].

Optical detection has several advantages. Firstly, the method is noninvasive and does not require an electrical connection. Secondly, optical sensors have high SNR and are not affected by electromagnetic interference, making them suitable for environments with high noise levels due to fast switching, especially with WBG devices [83]. Lastly, they have high bandwidth and can capture PD events during fast switching transients.

Despite these benefits, optical methods are often employed as supplementary "watchdogs" to other detection techniques like UHF and HFCT [15], [44], [83], [86]. This is primarily due to their inherent limitation in detecting internal PDs within the test specimen [79]. Even for surface PDs, the active area of sensors such as PMTs is relatively small [86]. Additionally, the method necessitates placing the specimen and optical sensor inside an enclosure with complete blackout. While this requirement is easily met for offline testing on twisted pairs or stator coils, it poses a challenge for adoption in online testing scenarios.

E. Software-Based Filtering and Post-Processing

IEC 60034-27-5 outlines using an analog high-order HPF to eliminate PWM harmonics from the PD spectrum. However, in the case of WBG devices with high slew rates, the switching noise spectrum extends up to the UHF range, bringing concern about overshadowing the PD spectrum, especially during the switching transition (dv/dt). To address this, the analog filter provides two provisions: increasing the slope (dB/decade) or raising the cut-off frequency to achieve higher attenuation for switching noise. Nevertheless, both solutions also result in higher attenuation of the PD spectrum, lowering detection sensitivity and accuracy.

Recently, software techniques based on Machine Learning have emerged as another way to augment the accuracy of PD detection under fast and ultra-fast switching rise time. A standard deviation-based algorithm is presented in [75], [96]. The method exploits the deterministic nature of the switching noise and the stochastic nature of PD. The switching noise pattern is similar for different switching instances, but PD noise pattern is random. A plot of the standard deviation of several switching transition time-domain acquisitions is plotted. The plot shows low standard deviation for the repetitive/similar switching noise but a significant standard deviation value for the random PD region. In other words, a high standard deviation value implies the occurrence of a PD event.

Similarly, in [97], a pattern recognition-based approach is proposed for detecting and estimating the intensity of high impedance PDs in twisted pairs under high dv/dt and voltage environment. The method involves measuring and post-processing the voltage across the resistor, placed in series with the twisted pair. When PD occurs, a distinctive impulse voltage with a peak proportional to the PD intensity is generated across the resistor. The DBSCAN algorithm is configured to detect these impulses and quantify the intensity by computing the charge based on the area under the impulse.

Further, an accuracy improvement method based on the Kalman Filter is proposed in [98]. The Kalman filter technique is shown to lessen variation and increase accuracy in PD localization. Similarly, an accurate detection through classification is proposed in [99] for PD detection in multi-level PWM. Trained classifiers based on ensemble bagged Decision Trees (DTs) and Long Short-Term Memory (LSTM) are built with $> 98\%$ accuracy. Lastly, the proposed model is shown to capture the temporal dependence of consecutive PDs.

V. Conclusion

Partial discharge poses a significant threat to the reliability of motors powered by Variable-Speed Pulse Width Modulation (VS-PWM) drives. The pulsating output shape of these drives stresses the stator winding, potentially leading to premature failure. For designing insulations that can withstand such challenges and ensure prolonged motor life, it is crucial to understand the impact of PWM characteristics, including rise time, frequency, and duty cycle, on PD activity within the motor winding. The aim of this study is to provide a comprehensive review of the literature investigating the impact of PWM characteristics on PD in motor windings.

Most studies twisted pair, following the IEC 60034-18-41 standard, with the rationale that the turn-to-turn location is the most vulnerable to PD. Among the PWM characteristics, rise time is a crucial factor influencing PD activity. However, a lack of consensus exists in the literature regarding its impact on PDIV, with varying opinions suggesting potential increases, decreases, or no change. Similar uncertainty prevails in studies analyzing the effects of frequency and duty cycle. Further, despite the crucial role of deadtime on drive performance, there is a notable scarcity of literature investigating its impact on PD.

Consequently, this study identifies the need for a definitive conclusion on the effect of each PWM characteristic on PD patterns. Establishing the most realistic understanding of the explanations and justifications presented in this paper is essential. Additionally, there is a call for further research on the impact of dead time on PD. Addressing these gaps in future studies could lay the groundwork for PD-free designs, especially in the context of WBG-based VS-PWM motor drives with fast and ultra-fast rise times.

Furthermore, the study also focuses on reviewing detection methods for PD in motor windings. Among the detection methods outlined in IEC 60034-27-5, electromagnetic couplers, being

non-invasive, are extensively researched and employed in literature for PD measurement in twisted pairs or stator windings, followed HFCTs. However, both HFCTs and electromagnetic couplers are susceptible to switching/EMI noise. Optical methods have recently gained popularity in assisting PD detection in studies examining the effects of high dv/dt in SiC-based drives. Lastly, while the current PD detection methods are based on offline detection, there is a call for developing standards and techniques for online PD detection in motors fed with next-generation WBG-based VS-PWM motor drives.

REFERENCES

[1] C. M. Martinez, X. Hu, D. Cao, E. Velenis, B. Gao, and M. Wellers, "Energy management in plug-in hybrid electric vehicles: Recent progress and a connected vehicles perspective," *IEEE Trans. Veh. Technol.*, vol. 66, no. 6, pp. 4534–4549, Jun. 2017.

[2] S. M. R. Borghei, "The modeling of partial discharge under fast, repetitive voltage pulses using finite-element analysis" Master's thesis, Virginia Polytechnic Institute and State University, 2020. [Online]. Available: https://vtechworks.lib.vt.edu/items/4facb80e-28f7-47f0-a663-7474b1bdcc4c

[3] V. Madonna, "Physics of failure as a technology enabler for electrical machines in transportation: Reliability-oriented design of low voltage insulation systems," Ph.D. dissertation, University of Nottingham, Nottingham, U.K., 2020. [Online]. Available: https://eprints.nottingham.ac.uk/60441/

[4] S. Kouro, J. Rodriguez, B. Wu, S. Bernet, and M. Perez, "Powering the future of industry: High-power adjustable speed drive topologies," *IEEE Ind. Appl. Mag.*, vol. 18, no. 4, pp. 26–39, Jul./Aug. 2012.

[5] P. Palmer, X. Zhang, E. Shelton, T. Zhang, and J. Zhang, "An experimental comparison of GaN, SiC and Si switching power devices," in *Proc. 43rd Annu. Conf. IEEE Ind. Electron. Soc.*, 2017, pp. 780–785.

[6] S. Yin, K. J. Tseng, P. Tu, R. Simanjorang, and A. K. Gupta, "Design considerations and comparison of high-speed gate drivers for Si IGBT and SiC MOSFET modules," in *Proc. IEEE Energy Convers. Congr. Expo.*, 2016, pp. 1–8.

[7] J. Srijeeth, S. Mohanrajan, and A. Vijayakumari, "Performance comparison of Si-IGBT and SiC-MOSFET in an inverter application using DPT," in *Proc. IEEE 2nd Int. Conf. Smart Technol. Power, Energy Control (STPEC)*, Bilaspur, Chhattisgarh, India, 2021, pp. 1–5, doi: 10.1109/STPEC52385.2021.9718720

[8] Texas Instruments, Understanding motor driver current ratings. [Online]. Available: https://www.ti.com/lit/an/slyt801/slyt801.pdf?ts=1699545088815&ref_url=https%253A%252F%252Fwww.google.com%252F

[9] S. Yin, K. Tseng, R. Simanjorang, and P. Tu, "Experimental comparison of high-speed gate driver design for 1.2-kV/120-A Si IGBT and SiC MOSFET modules," *IET Power Electron.*, vol. 10, pp. 979–986, 2017.

[10] G. Stone, S. Campbell, and S. Tetreault, "Inverter-fed drives: Which motor stators are at risk?," *IEEE Ind. Appl. Mag.*, vol. 6, no. 5, pp. 17–22, Sep./Oct. 2000.

[11] S. Grzybowski and S. Bandaru, "Effect of frequency, temperature, and voltage on the lifetime characteristics of magnet wires under pulse voltages," in *Proc. IEEE Int. Conf. Solid Dielectrics*, 2004, pp. 876–879.

[12] D. Fabiani, G. Montanari, and A. Contin, "Aging acceleration of insulating materials for electrical machine windings supplied by PWM in the presence and in the absence of partial discharges," in *Proc. IEEE 7th Int. Conf. Solid Dielectrics*, 2001, pp. 283–286.

[13] M. Tozzi, A. Cavallini, and G. C. Montanari, "Monitoring off-line and on-line PD under impulsive voltage on induction motors - Part 1: Standard procedure," *IEEE Elect. Insul. Mag.*, vol. 26, no. 4, pp. 16–26, Jul./Aug. 2010.

[14] High-Voltage Test Techniques Partial Discharge Measurements, IEC 60270:2000 Standard, 2015. [Online]. Available: https://webstore.iec.ch/publication/1247

[15] L. Lusuardi, A. Rumi, A. Cavallini, D. Barater, and S. Nuzzo, "Partial discharge phenomena in electrical machines for the more electrical aircraft. Part II: Impact of reduced pressures and wide bandgap devices," *IEEE Access*, vol. 9, pp. 27485–27495, 2021.

[16] M. Kaufhold, H. Aninger, M. Berth, J. Speck, and M. Eberhardt, "Electrical stress and failure mechanism of the winding insulation in PWM-inverter-fed low-voltage induction motors," *IEEE Trans. Ind. Electron.*, vol. 47, no. 2, pp. 396–402, Apr. 2000.

[17] L. Saunders, G. Skibinski, S. Evon, and D. Kempkes, "Riding the reflected wave-IGBT drive technology demands new motor and cable considerations," in *Proc. IAS Petroleum Chem. Ind. Tech. Conf.*, 1996, pp. 75–84.

[18] Rotating Electrical Machines-Part 18–41: Partial Discharge Free Electrical Insulation Systems (Type I) Used in Rotating Electrical Machines Fed From Voltage Converters-Qualification and Quality Control Tests, IEC 60034-18-41 Standard, 2014. [Online]. Available: https://webstore.iec.ch/publication/118

[19] E. Persson, "Transient effects in application of PWM inverters to induction motors," *IEEE Trans. Ind. Appl.*, vol. 28, no. 5, pp. 1095–1101, Sep./Oct. 1992.

[20] *Rotating electrical machines - Part 18-42: Partial discharge resistant electrical insulation systems (Type II) used in rotating electrical machines fed from voltage converters - Qualification tests*, Standard IEC 60034-18-42:2017, 2017. [Online]. Available: https://webstore.iec.ch/publication/28040

[21] H. Xiong, J. Zhang, and A. Von Jouanne, "Control of variable frequency drive PWM to mitigate motor overvoltage due to double pulsing in reflected wave phenomenon," in *Proc. IEEE Energy Convers. Congr. Expo.*, 2018, pp. 6563–6570.

[22] M. Fenger, S. Campbell, and J. Pedersen, "Motor winding problems caused by inverter drives," *IEEE Ind. Appl. Mag.*, vol. 9, no. 4, pp. 22–31, Jul./Aug. 2003.

[23] X. Liu, P. Liu, T. Zhang, P. Yuan, and H. Zhu, "Detection method of inter-turn insulation defects of inverter-fed motors under induced impulse voltage," *IEEE Elect. Insul. Mag.*, vol. 37, no. 1, pp. 27–39, Jan./Feb. 2021.

[24] W. Yin, "Failure mechanism of winding insulations in inverter-fed motors," *IEEE Elect. Insul. Mag.*, vol. 13, no. 6, pp. 18–23, Nov./Dec. 1997.

[25] J. He, H. Chen, R. Katebi, N. Weise, and N. A. Demerdash, "Mitigation of uneven surge voltage stress on stator windings of induction motors fed by SiC-MOSFET-based adjustable speed drives," in *Proc. IEEE Int. Electric Machines Drives Conf.*, 2017, pp. 1–7.

[26] IEC 61934, IEC61934 electrical insulating materials and systems - electrical measurement of partial discharges (PD) under short rise time and repetitive voltage impulses, 2011.

[27] A. Cavallini, E. Lindell, G. C. Montanari, and M. Tozzi, "Off-line PD testing of converter-fed wire-wound motors: When IEC TS 60034-18-41 may fail?," *IEEE Trans. Dielectr. Electr. Insul.*, vol. 17, no. 5, pp. 1385–1395, Oct. 2010.

[28] S. S. Vala, A. B. Mirza, and F. Luo, "A review on partial discharge phenomenon in rotating machines operated using WBG motor drives," in *Proc. IEEE Transp. Electrific. Conf. Expo*, 2022, pp. 523–528.

[29] G. C. Stone, *Electrical Insulation for Rotating Machines: Design Evaluation Aging Testing and Repair*. Hoboken, NJ, USA: Wiley, vol. 8, 2014.

[30] J. Lahtinen, "Voltage stress on stator winding of AC machine fed by variable speed drive," Master's thesis, Aalto University, 2019. [Online]. Available: https://aaltodoc.aalto.fi/server/api/core/bitstreams/429bc853-9ae5-4975-8d07-dd8d7aabc5a1/content

[31] Z. Wei, "Partial discharge characteristics under square-wave voltage pulses with ultra-short rise times under various pressures," Ph.D. dissertation, Ohio State University, 2021. [Online]. Available: https://etd.ohiolink.edu/acprod/odb_etd/ws/send_file/send?accession=osu164152453637455&disposition=inline

[32] Y. Ji et al., "Moving towards partial discharge-free design of electrical machines for more electric aircraft applications," *iIEEE Trans. Transp. Electrific.*, vol. 9, no. 3, pp. 4668–4679, Sep. 2023.

[33] Winding Wires - Test Methods - Part 5: Electrical Properties, IEC Standard 60851-5 ed. IV, 2008. [Online]. Available: https://webstore.iec.ch/publication/3699

[34] P. Wang, A. Cavallini, G. C. Montanari, and G. Wu, "Effect of rise time on PD pulse features under repetitive square wave voltages," *IEEE Trans. Dielectr. Electr. Insul.*, vol. 20, no. 1, pp. 245–254, Feb. 2013.

[35] P. Wang, G. C. Montanari, and A. Cavallini, "Partial discharge phenomenology and induced aging behavior in rotating machines controlled by power electronics," *IEEE Trans. Ind. Electron.*, vol. 61, no. 12, pp. 7105–7112, Dec. 2014.

[36] A. Cavallini, E. Lindell, G. C. Montanari, and M. Tozzi, "Inception of partial discharges under repetitive square voltages: Effect of voltage waveform and repetition rate on PDIV and RPDIV," in *Proc. Annu. Rep. Conf. Elect. Insul. Dielectic Phenomena*, 2010, pp. 1–4.

[37] P. Wang, H. Xu, J. Wang, W. Wang, and A. Cavallini, "Effect of repetitive impulsive voltage duty cycle on partial discharge features and insulation endurance of enameled wires for inverter-fed low voltage machines," *IEEE Trans. Dielectr. Electr. Insul.*, vol. 24, no. 4, pp. 2123–2131, 2017.

[38] K. Kimura, S. Ushirone, T. Koyanagi, Y. Iiyama, S. Ohtsuka, and M. Hikita, "Study of PD behaviors on a crossed sample of magnet-wire with repetitive bipolar impulses for inverter-fed motor coil insulation," in *Proc. Annu. Rep. Conf. Elect. Insul. Dielectric Phenomena*, 2005, pp. 393–396.

[39] P. Wang, A. Cavallini, and G. C. Montanari, "The influence of repetitive square wave voltage parameters on enameled wire endurance," *IEEE Trans. Dielectr. Electr. Insul.*, vol. 21, no. 3, pp. 1276–1284, Jun. 2014.

[40] N. Hayakawa, F. Shimizu, and H. Okubo, "Estimation of partial discharge inception voltage of magnet wires under inverter surge voltage by volume-time theory," *IEEE Trans. Dielectr. Electr. Insul.*, vol. 19, no. 2, pp. 550–557, Apr. 2012.

[41] T. Hammarström, "Multi-rise time PWM: A way to reduce PD exposure in motor windings," *IEEE Trans. Dielectr. Electr. Insul.*, vol. 27, no. 2, pp. 613–621, Apr. 2020.

[42] M. Morikawa, N. Hayakawa, and H. Okubo, "Partial discharge inception and degradation characteristics of inverter-fed motor sample under surge voltage condition," in *Proc. Annu. Rep. Conf. Elect. Insul. Dielectric Phenomena*, 2005, pp. 426–429.

[43] A. Rumi, A. Cavallini, and L. Lusuardi, "Impact of WBG converter voltage rise-time and switching frequency on the PDIV of twisted pairs," in *Proc. IEEE 3rd Int. Conf. Dielectrics*, 2020, pp. 902–905.

[44] Z. Wei, H. You, P. Fu, B. Hu, and J. Wang, "Partial discharge inception characteristics of twisted pairs under single voltage pulses generated by silicon-carbide devices," *IEEE Trans. Transport. Electrific.*, vol. 8, no. 2, pp. 1674–1683, Jun. 2022.

[45] D. R. Meyer, A. Cavallini, L. Lusuardi, D. Barater, G. Pietrini, and A. Soldati, "Influence of impulse voltage repetition frequency on RPDIV in partial vacuum," *IEEE Trans. Dielectr. Electr. Insul.*, vol. 25, no. 3, pp. 873–882, Jun. 2018.

[46] Z. Wei, H. You, B. Hu, R. Na, and J. Wang, "Partial discharge behavior on twisted pair under ultra-short rise time square-wave excitations," in *Proc. IEEE Elect. Insul. Conf.*, 2019, pp. 493–496.

[47] Y. Kikuchi, J. Matsusue, F. Yamada, T. Okuda, and T. Nakamura, "Repetitive partial discharge phenomena on electrical motor coil windings under high-repetition nanosecond pulsed voltages driven by SiC MOSFET inverter," *IEEE Access*, vol. 11, pp. 68826–68835, 2023.

[48] V. Madonna, P. Giangrande, W. Zhao, H. Zhang, C. Gerada, and M. Galea, "Electrical machines for the more electric aircraft: Partial discharges investigation," *IEEE Trans. Ind. Appl.*, vol. 57, no. 2, pp. 1389–1398, Mar./Apr. 2021.

[49] G. W. P. Wang, Y. Luo, and G. Zhu, "Effect of repetitive square voltage frequency on partial discharge features," *Sci. China Technological Sci.*, vol. 56, pp. 1313–1321, 2013.

[50] M. Florkowski, P. Błaszczyk, and P. Klimczak, "Partial discharges in twisted-pair magnet wires subject to multilevel PWM pulses," *IEEE Trans. Dielectr. Electr. Insul.*, vol. 24, no. 4, pp. 2203–2210, 2017.

[51] X. Zhu, Y. Wang, H. Sun, and Y. Yin, "Effect of rise time on partial discharge and aging characteristics of polyimide under square wave voltage," in *Proc. IEEE 4th Int. Conf. Elect. Mater. Power Equip.*, 2023, pp. 1–4.

[52] L. Benmamas, P. Teste, E. Odic, G. Krebs, and T. Hamiti, "Contribution to the analysis of PWM inverter parameters influence on the partial discharge inception voltage," *IEEE Trans. Dielectr. Electr. Insul.*, vol. 26, no. 1, pp. 146–152, Feb. 2019.

[53] P. Wang and A. Cavallini, "The influence of repetitive square wave voltage parameters on PD statistical features," in *Proc. Annu. Rep. Conf. Elect. Insul. Dielectric Phenomena*, 2013, pp. 1282–1285.

[54] F. Guastavino, A. Dardano, A. Ratto, and E. Torello, "Partial discharge activity in presence of pulsed waveforms," in *Proc. Conf. Rec. IEEE Int. Symp. Elect. Insul.*, 2008, pp. 336–339.

[55] G. C. Montanari and P. Seri, "The effect of inverter characteristics on partial discharge and life behavior of wire insulation," *IEEE Elect. Insul. Mag.*, vol. 34, no. 2, pp. 32–39, Mar./Apr. 2018.

[56] M. Diab, W. Zhou, C. Emersic, X. Yuan, and I. Cotton, "Impact of PWM voltage waveforms on magnet wire insulation partial discharge in SiC-based motor drives," *IEEE Access*, vol. 9, pp. 156599–156612, 2021.

[57] F. Chierchie, E. E. Paolini, and L. Stefanazzi, "Dead-time distortion shaping," *IEEE Trans. Power Electron.*, vol. 34, no. 1, pp. 53–63, Jan. 2019.

[58] A. B. Mirza, A. I. Emon, S. S. Vala, and F. Luo, "A comprehensive analysis of current spikes in a split-phase inverter," in *Proc. IEEE Appl. Power Electron. Conf. Expo.*, 2022, pp. 1580–1585.

[59] A. Datta, A. Guha, and G. Narayanan, "An advanced gate driver for insulated gate bipolar transistors to eliminate dead-time induced distortions in inverter output," in *Proc. IEEE Int. Conf. Power Electron. Drives Energy Syst.*, 2014, pp. 1–6.

[60] N. Diao, X. Sun, C. Song, Q. Zhang, and Z. Zhang, "A multimodulation times SVPWM for dead-time effect elimination in three-level neutral point clamped converters," *IEEE Trans. Ind. Electron.*, vol. 68, no. 7, pp. 5476–5485, Jul. 2021.

[61] J. Huang and K. Li, "Eliminating common-mode voltage spikes caused by dead-time effect in three-phase inverters through symmetrical rotation reverse carriers," *IEEE Trans. Power Electron.*, vol. 36, no. 5, pp. 6056–6067, May 2021.

[62] S. Akram et al., "Pulse width modulation voltage source deadtime effect on partial discharge and lifetime of inverter-fed motor insulation," *High Voltage*, vol. 7, no. 6, pp. 1185–1193, 2022. [Online]. Available: https://ietresearch.onlinelibrary.wiley.com/doi/full/10.1049/hve2.12223

[63] J. Wang et al., "Novel repetitive square wave voltage generator used for the insulation evaluation of rotating machines driven by power electronics," *IEEE Trans. Dielectr. Electr. Insul.*, vol. 24, no. 4, pp. 2041–2049, 2017.

[64] Y. Ji et al., "Electrical machine design considering corona-resistant wire for more electric aircraft applications," *IEEE Trans. Transport. Electrific.*, vol. 9, no. 2, pp. 3192–3202, Jun. 2023.

[65] T. Petri, M. Keller, and N. Parspour, "The insulation resilience of inverter-fed low voltage traction machines: Review, challenges, and opportunities," *IEEE Access*, vol. 10, pp. 104023–104049, 2022.

[66] T. Billard, T. Lebey, P. Castelan, and Y. Deville, "Partial discharge monitoring in twisted pair using non-intrusive sensors: Numerical analysis," in *Proc. Annu. Rep. Conf. Elect. Insul. Dielectric Phenomena*, 2013, pp. 1286–1289.

[67] T. J. Hammarström, "Partial discharge characteristics at ultra-short voltage risetimes," *IEEE Trans. Dielectr. Electr. Insul.*, vol. 25, no. 6, pp. 2241–2249, Dec. 2018.

[68] M. S. Diab, W. Zhou, C. Emersic, X. Yuan, and I. Cotton, "Impact of PWM waveforms on partial discharge in SiC-based motor drives," in *Proc. 47th Annu. Conf. IEEE Ind. Electron. Soc.*, 2021, pp. 1–7.

[69] H. Chai, B. T. Phung, and S. Mitchell, "Application of UHF sensors in power system equipment for partial discharge detection: A review," *Sensors*, vol. 19, no. 5, 2019. Art. no. 1029, doi: 10.3390/s19051029.

[70] H. Wang, G. Xiao, L. Wang, Y. Pei, F. Yan, and Q. Yang, "A novel approach to partial discharge detection under repetitive unipolar impulsive voltage," *IEEE Trans. Ind. Electron.*, vol. 70, no. 11, pp. 11681–11691, Nov. 2023.

[71] IEC 60034-27-1:2017, Rotating electrical machines - Part 27-1: Off-line partial discharge measurements on the winding insulation, 2017. [Online]. Available: https://webstore.iec.ch/publication/29254

[72] IEC 60034-27-2:2012, Rotating electrical machines - Part 27-2: On-line partial discharge measurements on the stator winding insulation of rotating electrical machines, 2012. [Online]. Available: https://webstore.iec.ch/publication/131

[73] G. Stone and H. Sedding, "Comparison of low and high frequency partial discharge measurements on stator windings," in *Proc. Nordic Insul. Symp.*, 2019, pp. 134–138.

[74] C. Abadie, T. Billard, and T. Lebey, "Partial discharges in motor fed by inverter: From detection to winding configuration," *IEEE Trans. Ind. Appl.*, vol. 55, no. 2, pp. 1332–1341, Mar./Apr. 2019.

[75] R. Ghosh, P. Seri, and G. Montanari, "Measuring partial discharges under power electronics waveforms: From slow to ultra-fast voltage impulse risetime," in *Proc. IEEE 4th Int. Conf. Condition Assessment Techn. Elect. Syst.*, 2019, pp. 1–6.

[76] B. Hu et al., "A partial discharge study of medium-voltage motor winding insulation under two-level voltage pulses with high Dv/Dt," *IEEE Open J. Power Electron.*, vol. 2, pp. 225–235, 2021.

[77] IEC 60034-27-5:2021, Rotating electrical machines - Part 27-5: Off-line measurement of partial discharge inception voltage on winding insulation under repetitive impulse voltage, 2021. [Online]. Available: https://webstore.iec.ch/publication/31870

[78] K. Kimura, "The role of IEC 60034-27-5 for IEC 60034-18-41: Offline PD test methods with repetitive impulse voltage," in *Proc. Int. Symp. Elect. Insulating Mater.*, 2017, pp. 155–158.

[79] *IEEE Recommended Practice for Quality Control Testing of External Discharges on Stator Coils, Bars, and Windings*, IEEE Standard 1799-2022 (Revision of IEEE Standard 1799-2012), pp. 1–52, 2022. [Online]. Available: https://standards.ieee.org/ieee/1799/7751/

[80] S. Biswas, C. Koley, B. Chatterjee, and S. Chakravorti, "A methodology for identification and localization of partial discharge sources using optical sensors," *IEEE Trans. Dielectr. Electr. Insul.*, vol. 19, no. 1, pp. 18–28, Feb. 2012.

[81] G. Stone, M. K. Stranges, and D. G. Dunn, "Common questions on partial discharge testing: A review of recent developments in IEEE and IEC standards for offline and online testing of motor and generator stator windings," *IEEE Ind. Appl. Mag.*, vol. 22, no. 1, pp. 14–19, Jan./Feb. 2016.
[82] G. C. Stone, H. G. Sedding, and C. Chan, "Experience with online partial-discharge measurement in high-voltage inverter-fed motors," *IEEE Trans. Ind. Appl.*, vol. 54, no. 1, pp. 866–872, Jan./Feb. 2018.
[83] H. Sun, Y. Wang, Y. Ding, Y. Rui, L. Fan, and Y. Yin, "Partial discharge detection of electrical machine insulation under PWM voltage with high dV/dT for more electric aircraft," in *Proc. IEEE Energy Convers. Congr. Expo.*, 2022, pp. 1–5.
[84] S. Akram, X. Liu, P. Wang, P. Meng, J. Castellon, and A. Cavallini, "Design of a rectangular wave high voltage generator for the evaluation of inverter-fed motor insulation," *IEEE Trans. Ind. Electron.*, vol. 70, no. 5, pp. 4485–4493, May 2023.
[85] J. M. Martínez-Tarifa and G. Robles, "Partial discharges measurement during under-damped steep-fronted overvoltages," in *Proc. IEEE Int. Instrum. Meas. Technol. Conf.*, 2020, pp. 1–5.
[86] H. Xiong et al., "The Ohio State University partial discharge detection platform for electric machine windings driven by PWM voltage excitation," in *Proc. IEEE Elect. Insul. Conf.*, 2019, pp. 517–520.
[87] Y. Shibuya, S. Matsumoto, M. Tanaka, H. Muto, and Y. Kaneda, "Electromagnetic waves from partial discharges and their detection using patch antenna," *IEEE Trans. Dielectr. Electr. Insul.*, vol. 17, no. 3, pp. 862–871, Jun. 2010.
[88] S. Ma, P. Wang, and Y. Zhu, "A novel PD detection method for inverter-fed motor using shell as slot antenna," in *Proc. IEEE 4th Int. Conf. Elect. Mater. Power Equip.*, 2023, pp. 1–4.
[89] T. Yamada, K. Takagi, M. Fujieda, Y. Takahashi, and Y. Hayashi, "Measurement of voltage distribution and partial discharge position in inverter-fed rectangular wire motor," in *Proc. IEEE Conf. Elect. Insul. Dielectric Phenomena*, 2021, pp. 570–573.
[90] T. Billard et al., "Using non-intrusive sensors to detect partial discharges in a PWM inverter environment: A twisted pair example," in *Proc. IEEE Elect. Insul. Conf.*, 2013, pp. 329–332.
[91] Y. Wang, Z. Yuan, H. Peng, Y. Ding, Y. Yin, and L. Fang, "Partial discharge testing platform for high voltage power module packaging under square wave excitation," in *Proc. IEEE Appl. Power Electron. Conf. Expo.*, 2021, pp. 1491–1495.
[92] J. V. Klüss and A.-P. Elg, "Challenges associated with implementation of HFCTs for partial discharge measurements," in *Proc. Conf. Precis. Electromagn. Meas.*, 2020, pp. 1–2.
[93] Z. Guo, A. Q. Huang, R. E. Hebner, G. C. Montanari, and X. Feng, "Characterization of partial discharges in high-frequency transformer under PWM pulses," *IEEE Trans. Power Electron.*, vol. 37, no. 9, pp. 11199–11208, Sep. 2022.
[94] G. Cleary and M. Judd, "UHF and current pulse measurements of partial discharge activity in mineral oil," *IEE Proc. Science, Meas. Technol.*, vol. 153, pp. 47–54, Mar. 2006. [Online]. Available: https://digital-library.theiet.org/content/journals/10.1049/ip-smt_20050103
[95] K. Tang, J. Tao, Y. Yan, J. Chen, and X. Yue, "Realization of Rogowski coil for partial discharge measurement," in *Proc. 6th Int. Conf. Power Renewable Energy*, 2021, pp. 46–50.
[96] G. C. Montanari, R. Hebner, P. Seri, and R. Ghosh, "Noise rejection and partial discharge identification in PDIV tests of insulated wires under repetitive impulse supply voltage," in *Proc. IEEE Elect. Insul. Conf.*, 2019, pp. 505–508.
[97] K. Choksi, S. Salehi, A. B. Vala Mirza, and F. Luo, "Comprehensive evaluation and detection of partial discharge in WBG motor drive using DBscan based feature extraction," in *Proc. IEEE Energy Convers. Congr. Expo.*, 2023, pp. 1–7.
[98] P. Shen, T. Chen, D. Tang, T. He, L. Ju, and H. Wang, "The accuracy improvement method for partial discharge UHF measurement data based on Kalman filter algorithm," in *Proc. Power System Green Energy Conf.*, 2022, pp. 1082–1086.
[99] E. Balouji, T. Hammarström, and T. McKelvey, "Classification of partial discharges originating from multilevel PWM using machine learning," *IEEE Trans. Dielectr. Electr. Insul.*, vol. 29, no. 1, pp. 287–294, Feb. 2022.

Sama Salehi Vala (Graduate Student Member, IEEE) received the B.Sc. and M.Sc. degrees in electrical engineering from the University of Tabriz, Tabriz, Iran, in 2014 and 2018, respectively. She is currently working toward the Ph.D. degree in electrical engineering with the Stony Brook University, Stony Brook, NY, USA. Her research interests include the design and analysis of power electronics converters, motor drives, high-voltage power module packaging, renewable energy systems, reliability, and partial discharge partial discharge mechanisms in medium voltage motors driven by motor drives, and semiconductor devices under diverse environmental conditions.

Abdul Basit Mirza (Graduate Student Member, IEEE) received the bachelor's degree (with Hons.) in electrical engineering (Power) from the University of Engineering and Technology, Lahore, Pakistan, in 2018, and the master's degree in 2022 from Stony Brook University, Stony Brook, NY, USA, with a concentration in MVDC breakers using WBG-based power electronics. He is currently working toward the Ph.D. degree in electrical engineering with Stony Brook University. He is currently a graduate Research Assistant and involved in research projects with the Oak Ridge National Laboratory (ORNL), Oak Ridge, TN, USA, and Federal Aviation Administration. In 2022, he was a research Intern with GE Global Research, Niskayuna, NY, USA. His research interests include system level design of high-density Wide Band Gap based power converters and electromagnetic interference and compatibility characterization.

Asif Imran Emon (Member, IEEE) received the B.Sc. degree in electrical and electronic engineering from the Chittagong University of Engineering and Technology, Chittagong, Bangladesh, in 2015, the M.S. degree from the University of Arkansas, Fayetteville, AR, USA, and the Ph.D. degree from the State University of New York, Stony Brook, NY, USA, in 2020 and 2022, respectively. He interned at GE Global Research, Niskayuna, NY, during the summer of 2021. In 2022, he was an EMC design engineering team Intern with Apple Inc., Cupertino, CA, USA. His research interests include power module packaging of wide band-gap devices, efficient energy conversion and electromagnetic interference and compatibility analysis in motor drives.

Fang Luo (Senior Member, IEEE) received the bachelor's and Ph.D. degrees from the Huazhong University of Science and Technology, Wuhan, China, and jointly from Virginia Tech, Blacksburg, VA, USA, in 2003 and 2010, respectively. He was an Assistant Professor with the Electrical Engineering Department, University of Arkansas, Fayetteville, AR, USA, from 2017 to 2020, and a Research Assistant Professor with The Ohio State University, Columbus, OH, USA, from 2014 to 2017. He was a Visiting Ph.D. Student from 2007 to 2010 and then a Postdoctoral Researcher from 2010 to 2014 with Virginia Tech. He is currently an Empire Innovation Associate Professor and the Director of the Spellman High Voltage Laboratory, Stony Brook University (SUNY Stony Brook), Stony Brook, NY, USA, with his background in power electronics. His research interests include high power density converter design, high-density electromagnetic interference filter design and integration, and power module packaging/integration for wide bandgap devices. Dr. Luo is also a Member of American Institute of Aeronautics and Astronautics and American Society of Mechanical Engineers. He was the recipient of the NSF CAREER Award.